OPEN ACCESS Freely available online

PLoS one

Inhibition of G Protein-Activated Inwardly Rectifying K^+ Channels by Different Classes of Antidepressants

Toru Kobayashi[1,2]*, Kazuo Washiyama[1], Kazutaka Ikeda[2]

1 Department of Project Programs, Center for Bioresource-based Researches, Brain Research Institute, Niigata University, Niigata, Japan, **2** Research Project for Addictive Substances, Tokyo Metropolitan Institute of Medical Science, Tokyo, Japan

Abstract

Various antidepressants are commonly used for the treatment of depression and several other neuropsychiatric disorders. In addition to their primary effects on serotonergic or noradrenergic neurotransmitter systems, antidepressants have been shown to interact with several receptors and ion channels. However, the molecular mechanisms that underlie the effects of antidepressants have not yet been sufficiently clarified. G protein-activated inwardly rectifying K^+ (GIRK, Kir3) channels play an important role in regulating neuronal excitability and heart rate, and GIRK channel modulation has been suggested to have therapeutic potential for several neuropsychiatric disorders and cardiac arrhythmias. In the present study, we investigated the effects of various classes of antidepressants on GIRK channels using the *Xenopus* oocyte expression assay. In oocytes injected with mRNA for GIRK1/GIRK2 or GIRK1/GIRK4 subunits, extracellular application of sertraline, duloxetine, and amoxapine effectively reduced GIRK currents, whereas nefazodone, venlafaxine, mianserin, and mirtazapine weakly inhibited GIRK currents even at toxic levels. The inhibitory effects were concentration-dependent, with various degrees of potency and effectiveness. Furthermore, the effects of sertraline were voltage-independent and time-independent during each voltage pulse, whereas the effects of duloxetine were voltage-dependent with weaker inhibition with negative membrane potentials and time-dependent with a gradual decrease in each voltage pulse. However, Kir2.1 channels were insensitive to all of the drugs. Moreover, the GIRK currents induced by ethanol were inhibited by sertraline but not by intracellularly applied sertraline. The present results suggest that GIRK channel inhibition may reveal a novel characteristic of the commonly used antidepressants, particularly sertraline, and contributes to some of the therapeutic effects and adverse effects.

Citation: Kobayashi T, Washiyama K, Ikeda K (2011) Inhibition of G Protein-Activated Inwardly Rectifying K^+ Channels by Different Classes of Antidepressants. PLoS ONE 6(12): e28208. doi:10.1371/journal.pone.0028208

Editor: Kenji Hashimoto, Chiba University Center for Forensic Mental Health, Japan

Received September 1, 2011; **Accepted** November 3, 2011; **Published** December 2, 2011

Funding: This work was supported by research grants from the Ministry of Education, Culture, Sports Science and Technology of Japan and the Ministry of Health, Labour and Welfare of Japan. The funders had no role in study design, data collection and analysis, decision to publish, or preparation of the manuscript.

Competing Interests: The authors have declared that no competing interests exist.

* E-mail: torukoba@bri.niigata-u.ac.jp

Introduction

Depression is one of the most common illnesses in the world [1,2]. After the efficacy of tricyclic antidepressants (TCAs), including imipramine, amitriptyline and amoxapine, was well established, various classes of antidepressants were introduced, including selective serotonin reuptake inhibitors (SSRIs; fluoxetine, paroxetine and sertraline), serotonin-norepinephrine reuptake inhibitors (SNRIs; venlafaxine and duloxetine), selective norepinephrine reuptake inhibitors (NRIs; reboxetine), noradrenergic and specific serotonergic antidepressants (NaSSAs; mirtazapine and mianserin), and 5-hydroxytryptamine type 2 (5-HT_2) receptor antagonists (nefazodone) [1–3]. Antidepressants are commonly used for the treatment of depression and several neuropsychiatric disorders, such as anxiety disorders, eating disorders, obsessive-compulsive disorders, and chronic pain disorders [1–3]. Their clinical efficacy is hypothesized to be linked mainly with facilitation of noradrenergic or serotonergic function in the brain [2]. In contrast, the interaction between antidepressants and muscarinic, α_1 adrenergic, and H_1 histamine receptors is involved in some of their adverse side effects, such as dry mouse, orthostatic hypotension, and sedation [2]. Antidepressants have also been shown to modulate the function of several other receptors and ion channels, including 5-HT_{2C} and 5-HT_3 receptors, nicotinic acetylcholine receptors, *N*-methyl-D-aspartate (NMDA) receptor channels, $P2X_2$ receptors, voltage-gated Ca^{2+}, Na^+, and K^+ channels, Ca^{2+}-activated K^+ channels, two-pore-domain K^+ channels, and volume regulated anion channels [4–23]. The modulation of these receptors and channels might also be relevant to the pharmacological effects of antidepressants. However, the molecular mechanisms that underlie the effects of various antidepressants have not yet been sufficiently clarified.

G protein-activated inwardly rectifying K^+ (GIRK) channels (also known as Kir3 channels) are members of a major subfamily of inwardly rectifying K^+ (Kir) channels that includes seven subfamilies [24]. Four GIRK channel subunits have been identified in mammals [25–27]. Neuronal GIRK channels are predominantly heterotetramers composed of GIRK1 and GIRK2 subunits in most brain regions or homotetramers composed of GIRK2 subunits in the substantia nigra [27–30], whereas atrial GIRK channels are heterotetramers composed of GIRK1 and GIRK4 subunits [26]. The channels are activated by various $G_{i/o}$-protein-coupled receptors, such as M_2 muscarinic, α_2 adrenergic, D_2 dopaminergic, opioid, nociceptin/orphanin FQ, CB_1 cannabinoid, and A_1 adenosine receptors, through the direct action of G-protein $\beta\gamma$ subunits [31–33]. Additionally, ethanol activates GIRK

channels independently of G-protein-coupled signaling pathways [34,35]. GIRK channels play an important role in regulating neuronal excitability, synaptic transmission, and heart rate [31,36–39]. Furthermore, recent studies have suggested that GIRK channel modulation has the potential for treating several neuropsychiatric disorders and cardiac arrhythmias [33,40,41]. Therefore, GIRK channel modulators may affect various brain and cardiac functions. We have demonstrated the distinctive effects of several antidepressants on GIRK channels, even among the same class, particularly SSRIs [42,43]. To further clarify the interaction between various classes of commonly used antidepressants and GIRK channels may be useful for advancing our understanding of the pharmacological effects of antidepressants. In the present study, we examined the effects of various antidepressants on GIRK channels using the *Xenopus* oocyte expression assay.

Materials and Methods

Preparation of specific mRNAs

Plasmids that contain the entire coding sequences for the mouse GIRK1, GIRK2, and GIRK4 channel subunits were obtained previously [34,44,45]. cDNAs for mouse Kir2.1 in pcDNA1 [46] were generously provided by Dr. Lily Y. Jan (University of California, San Francisco). These plasmids were linearized by digestion with the appropriate enzymes as described previously [45,46]. The specific mRNAs were synthesized *in vitro* using the mMESSAGE mMACHINE™ *In Vitro* Transcription Kit (Ambion, Austin, TX, USA).

Electrophysiological analysis

Adult female *Xenopus laevis* frogs (Copacetic, Soma, Aomori, Japan) were anesthetized by immersion in water that contained 0.15% tricaine (Sigma-Aldrich, St. Louis, MO, USA). A small incision was made on the abdomen to remove several ovarian lobes from the frogs, which were humanely killed after the final collection. All procedures for the care and treatment of animals were performed in accordance with National Institutes of Health guidelines and were approved by the Institutional Animal Care and Use Committee of Niigata University (Permit Number: 172-2). *Xenopus* oocytes (Stages V and VI) were manually isolated from the ovary and maintained in Barth's solution [47]. Oocytes were injected with mRNA for GIRK1/GIRK2 or GIRK1/GIRK4 combinations (0.15 ng each) or Kir2.1 (0.3 ng). The oocytes were incubated at 19°C in Barth's solution and manually defolliculated after treatment with 0.8 mg/ml collagenase (Wako Pure Chemical Industries, Osaka, Japan) for 1 h. The whole-cell currents of the oocytes were recorded from 3 to 9 days after injection with a conventional two-electrode voltage clamp [34,48]. The membrane potential was held at −70 mV unless otherwise specified. Microelectrodes were filled with 3 M KCl. The oocytes were placed in a 0.05 ml narrow chamber and continuously superfused with a high-potassium (hK) solution (96 mM KCl, 2 mM NaCl, 1 mM $MgCl_2$, 1.5 mM $CaCl_2$ and 5 mM HEPES, pH 7.4 with KOH) or a K^+-free high-sodium (ND98) solution (98 mM NaCl, 1 mM $MgCl_2$, 1.5 mM $CaCl_2$ and 5 mM HEPES, pH 7.4 with NaOH) at a flow rate of 2.5 ml/min. In the hK solution, the K^+ equilibrium potential was close to 0 mV, and the inward K^+ current flow through the Kir channels was observed at negative holding potentials as previously shown [25,27,43]. Additionally, to examine the effects of antidepressants on outward K^+ currents, a perfusion solution that contained 4 mM K^+ (K4 solution) was made by substituting NaCl with KCl in the ND98 solution. To examine the effects of an antidepressant on GIRK channels activated by G-protein activation, 13.8 nl of 100 mM Li_4-guanosine-5′-*O*-(3-thiotriphosphate) (GTPγS; Sigma-Aldrich), a nonhydrolyzable G-protein activator, dissolved in distilled water was injected into an oocyte using a nanoliter injector (World Precision Instruments, Sarasota, FL, USA) as described previously [49]. Furthermore, to examine the effects of intracellular sertraline, 23 nl of 10 mM sertraline dissolved in distilled water was injected into an oocyte using a Nanoliter injector as described previously [50], and the oocyte currents were then continuously recorded for approximately 30–40 min. Because the volume of the *Xenopus* oocytes used was approximately 1 µl, the intracellular concentration of sertraline was presumed to be approximately 225 µM. For the analysis of concentration-response relationships, the data were fitted to a standard logistic equation [51] using KaleidaGraph (Synergy Software, Reading, PA, USA). The concentration of a drug that produces 50% of the maximal current response for that drug (EC_{50}), the concentrations required to reduce control currents by 25% and 50% (IC_{25} and IC_{50}, respectively), and the Hill coefficient (n_H) were obtained from the concentration-response relationships.

Data analyses

The data are expressed as mean ± SEM, and n is the number of oocytes tested. The statistical analysis of differences between groups was performed using paired t-test, one-way analysis of variance (ANOVA), or two-way ANOVA followed by the Tukey-Kramer *post hoc* test. Values of $P<0.05$ were considered statistically significant.

Compounds

All of the antidepressants tested were commercially purchased. Amoxapine and nefazodone hydrochloride were obtained from Sigma-Aldrich. Mirtazapine and mianserin hydrochloride were obtained from Tocris Bioscience (Bristol, UK). Sertraline hydrochloride and duloxetine hydrochloride were obtained from Tronto Research Chemicals (North York, Canada). Venlafaxine hydrochloride was obtained from LKT Laboratories (St. Paul, MN, USA). Sertraline was dissolved in dimethyl sulfoxide (DMSO) or distilled water, and venlafaxine was dissolved in distilled water. The other antidepressants were dissolved in DMSO. The stock solution of each compound was stored at −30°C until use. Ethanol was purchased from Wako Pure Chemical Industries. Each compound was added to the perfusion solution in appropriate amounts immediately before the experiments.

Results

Inhibition of GIRK channels by antidepressants

In *Xenopus* oocytes injected with GIRK1 and GIRK2 mRNAs, basal GIRK currents, which depend on free G-protein βγ subunits present in the oocytes because of the inherent activity of G-proteins [32], were observed at a holding potential of −70 mV in an hK solution that contained 96 mM K^+ (Fig. 1A). The 3 mM Ba^{2+}-sensitive current components (1042.8±90.1 nA, $n=30$) correspond to the magnitude of GIRK currents in oocytes that express GIRK channels [34]. Extracellular application of 30 µM sertraline, an SSRI, reversibly reduced the inward currents through the expressed GIRK channels (Fig. 1A). The current responses to an additional 100 µM sertraline during the application of 3 mM Ba^{2+}, which blocks Kir channels, were not significant (reduction of inward currents by 4.5±3.5 nA; less than 1% inhibition of the Ba^{2+}-sensitive current components, $n=4$). Sertraline at 100 µM produced no significant response in a K^+-free ND98 perfusion solution that contained 98 mM Na^+ instead of the hK solution (3.0±1.8 nA, $n=4$), suggesting that the SSRI-sensitive current components show K^+ selectivity. Additionally, the application of DMSO or distilled water, the solvent vehicles, at the

highest concentration (0.3%) induced no significant current response in the hK or ND98 solutions ($n=5$; data not shown). In contrast, in oocytes injected with mRNA for Kir2.1, a constitutively active Kir channel [46], extracellular application of 300 μM sertraline had no significant effect on the inward currents through the channels in the hK solution (less than 2% change of the Ba^{2+}-sensitive current components; 848.3±322.0 nA, $n=4$; Fig. 1B). In uninjected oocytes, 300 μM sertraline and 3 mM Ba^{2+} caused no significant response (2.0±2.0 nA, $n=4$, and 3.1±1.7 nA, $n=4$, respectively; Fig. 1C) compared with oocytes injected with GIRK mRNA, suggesting no significant effect of sertraline or Ba^{2+} on intrinsic oocyte channels. Furthermore, in oocytes injected with GIRK1 and GIRK4 mRNAs, 30 μM sertraline similarly inhibited basal GIRK currents under the same conditions (51.6±4.3% inhibition of 3 mM Ba^{2+}-sensitive current components, 561.7±58.2 nA, $n=11$). Additionally, the Ba^{2+}-sensitive current components in oocytes injected with mRNA for GIRK1/GIRK2 or GIRK1/GIRK4 combinations were very significantly larger than those in oocytes injected with the same small amount of a single GIRK mRNA (less than 20 nA, $n=7$, respectively). The results indicate that sertraline predominantly inhibited GIRK1/2 and GIRK1/4 heteromultimeric channels, but not Kir2.1 channels. Moreover, the effects of different classes of antidepressants on GIRK channels were examined using the same expression assay. Amoxapine, a second generation TCA, and duloxetine, an SNRI, significantly inhibited basal GIRK currents at 100 μM (45.6±4.4 and 65.6±1.0% inhibition for GIRK1/2, $n=5$ and 7, respectively; 27.6±4.0 and 49.7±2.2% inhibition for GIRK1/4, $n=4$ and 6, respectively). However, the 5-HT_2 receptor antagonist nefazodone, NaSSAs mianserin and mirtazapine, and SNRI venlafaxine weakly inhibited the currents at 100 μM (35.9±3.5, 24.1±5.5, 17.6±3.5, and 19.4±4.6% inhibition for GIRK1/2, $n=11$, 4, 4, and 4, respectively; 30.3±3.4, 18.8±1.3, 12.1±2.4, and 22.8±3.2% inhibition for GIRK1/4, $n=13$, 5, 5, and 5, respectively). Additionally, the inhibitions were reversible with washout, similar to sertraline (data not shown). In contrast, Kir2.1 channels were insensitive to these drugs at 100 μM (less than 4% change of the Ba^{2+}-sensitive current components; 912.5±182.8 nA, $n=4$). In uninjected oocytes, 300 μM of the drugs caused no significant response (less than 6 nA; $n=4$ for each of the drugs). Altogether, the results suggest significant inhibition of GIRK channels by sertraline, duloxetine, and amoxapine, weak inhibition of the channels by nefazodone, mianserin, mirtazapine, and venlafaxine, and no significant effects of the drugs on Kir2.1 channels.

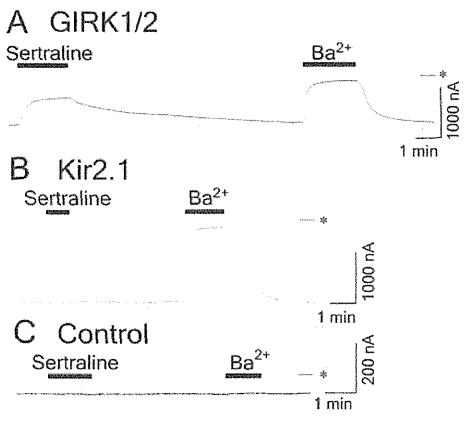

Figure 1. Inhibitory effects of sertraline on GIRK channels expressed in *Xenopus* oocytes. (A) In an oocyte injected with GIRK1 and GIRK2 mRNAs, current responses to 30 μM sertraline and 3 mM Ba^{2+} are shown. (B) In an oocyte injected with Kir2.1 mRNA, current responses to 100 μM sertraline and 3 mM Ba^{2+} are shown. (C) In an uninjected oocyte, no significant current responses to 300 μM sertraline or 3 mM Ba^{2+} are shown. Current responses were measured at a membrane potential of −70 mV in an hK solution that contained 96 mM K^+. Asterisks show the zero current level. Horizontal bars indicate the duration of application.
doi:10.1371/journal.pone.0028208.g001

Concentration-dependent inhibition of GIRK channels by various antidepressants

The concentration-response relationships for the inhibitory effects of different classes of antidepressants on GIRK1/2 and GIRK1/4 channels were investigated. Figure 2 shows that the inhibitions of both types of GIRK channels by various antidepressants were concentration-dependent with distinctive potency and effectiveness at micromolar concentrations. The rank order of the inhibition of GIRK channels by 100 μM of these drugs was the following: duloxetine≥sertraline>amoxapine>nefazodone>mianserin≥venlafaxine≈mirtazapine for GIRK1/2 channels and sertraline>duloxetine≫nefazodone, amoxapine>venlafaxine, mianserin>mirtazapine for GIRK1/4 channels. Table 1 shows the EC_{50} and n_H values obtained from the concentration-response relationships for sertraline, duloxetine and amoxapine, and the percentage inhibition of the GIRK currents by the drugs at the highest concentrations tested. Additionally, because the drugs could not completely block these types of GIRK channels even at the highest concentrations tested, the IC_{25} and IC_{50} values were also calculated to further compare the effects of the drugs (Table 1). The inhibition of GIRK1/2 channels by sertraline was similar to that by duloxetine (Fig. 2). Furthermore, the inhibition of GIRK1/2 channels by sertraline was statistically similar to the inhibition of GIRK1/4 channels ($P>0.05$ at each concentration, Tukey-Kramer *post hoc* test; Fig. 2, Table 1). In contrast, the inhibition of GIRK1/2 channels by duloxetine and amoxapine was more effective than the inhibition of GIRK1/4 channels ($P<0.05$ at 30, 100, and 300 μM for duloxetine and $P<0.05$ at 300, 500, and 1000 μM for amoxapine, Tukey-Kramer *post hoc* test; Fig. 2, Table 1).

Characteristics of inhibition of GIRK channels by the SSRI sertraline and SNRI duloxetine

Sertraline and duloxetine, which belong to commonly used classes of antidepressants, effectively inhibited GIRK channels, and we further investigated the effects of these drugs in more detail. Instantaneous GIRK1/2 currents elicited by the voltage step to −100 mV from a holding potential of 0 mV were diminished in the presence of 30 μM sertraline applied for 3 min (Fig. 3A). The percentage inhibition of the steady-state GIRK current at the end of the voltage step by sertraline was not significantly different from that of the instantaneous current ($P>0.05$, paired t-test; $n=9$ at −40, −60, −80, −100, and −120 mV, respectively). For duloxetine, the instantaneous currents were primarily diminished in the presence of 30 μM duloxetine, and the currents gradually increased in the voltage step (Fig. 3A). The percentage inhibition of the steady-state GIRK current at the end of the voltage step by duloxetine significantly decreased compared with that of the instantaneous current ($P<0.05$ at −80, −100 and −120 mV, paired t-test, $n=6$). Figure 3B shows that 30 μM sertraline- and duloxetine-sensitive currents in oocytes that expressed GIRK1/2 channels increased with negative membrane potentials, and the current-voltage relationships showed strong inward rectification ($n=9$ and 6,

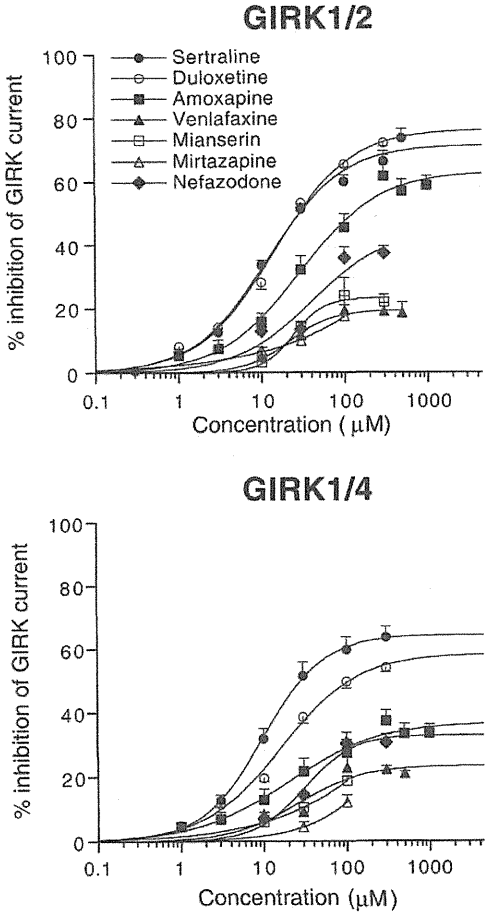

Figure 2. Concentration-response relationships for the effects of various antidepressants on GIRK1/2 and GIRK1/4 channels. The magnitudes of inhibition of GIRK currents by the drugs were compared with the 3 mM Ba^{2+}-sensitive current components in oocytes that expressed GIRK1/2 channels or GIRK1/4 channels (762.8±36.0 nA, $n=50$, and 585.0±44.0 nA, $n=40$, respectively). Each point and error bar represent the mean ± SEM of the percentage responses.
doi:10.1371/journal.pone.0028208.g002

respectively), similar to 3 mM Ba^{2+}-sensitive currents that corresponded to basal GIRK currents, indicating a characteristic of GIRK currents. The percentage inhibition of GIRK1/2 currents by 30 μM sertraline at the end of the voltage pulses showed no significant difference across voltages between −120 and −40 mV (no significant sertraline effect×membrane potential effect interaction, $P>0.1$, one-way ANOVA; $P>0.1$ across voltages, Tukey-Kramer *post hoc* test; Fig. 3C), suggesting voltage-independent inhibition of GIRK channels by sertraline. In contrast, the GIRK current inhibition by duloxetine at the end of the voltage pulses was voltage-dependent, with weaker inhibition at more negative membrane potentials (significant duloxetine effect×membrane potential effect interaction, $P<0.05$, one-way ANOVA; significant differences between −120 and −60 mV, between −120 and −40 mV, between −100 and −60 mV, and between −100 and −40 mV, $P<0.05$, Tukey-Kramer *post hoc* test, $n=6$, Fig. 3C). The voltage-dependency was associated with a time-dependent decrease in the inhibition by duloxetine in the voltage pulses at more negative membrane potentials. Furthermore, similar results were obtained in oocytes that expressed GIRK1/4 channels ($n=4$ for each of the drugs; data not shown). Altogether, sertraline and duloxetine primarily inhibited GIRK channels at the holding potential of 0 mV before the voltage pulses. The inhibitory effects of sertraline were voltage-independent and time-independent during each voltage pulse, whereas those of duloxetine decreased voltage-dependently with negative membrane potentials and time-dependently up to a steady state current level in each voltage pulse.

Furthermore, the effects of the two antidepressants on GIRK channels under a physiological K^+ condition were examined. In oocytes injected with GIRK1 and GIRK2 mRNAs, outward currents observed at a holding potential of −10 mV in a K4 solution that contained 4 mM K^+ were reversibly reduced by 30 μM sertraline ($n=4$), 30 μM duloxetine ($n=4$), and 3 mM Ba^{2+} (the Ba^{2+}-sensitive current components, 49.0±2.8 nA, $n=8$; Fig. S1), whereas in uninjected oocytes, the drugs at 100 μM and 3 mM Ba^{2+} caused no significant response (3.0±0.9 nA for sertraline, 0±0 nA for duloxetine, and 7.6±1.3 nA for Ba^{2+}; $n=4$, 4, and 8, respectively). The results suggest that the antidepressants also inhibited outward GIRK currents at a physiologically extracellular K^+ concentration.

Sertraline and duloxetine possess a secondary amine group with pK_a values of 8.9 and 9.34, respectively (Data Sheets of Pfizer and

Table 1. Inhibitory effects of sertraline, duloxetine and amoxapine on GIRK channels.

	Sertraline		*Duloxetine*		*Amoxapine*	
	GIRK1/2	**GIRK1/4**	**GIRK1/2**	**GIRK1/4**	**GIRK1/2**	**GIRK1/4**
EC_{50} (μM)	11.7±1.0	12.6±2.5	14.9±0.4	17.0±1.3	38.7±6.2	17.7±4.4
IC_{25} (μM)	6.9±0.6	7.0±1.0	6.6±0.6	12.6±1.2	21.5±8.3	39.7±15.8
IC_{50} (μM)	29.1±3.4	36.7±7.8	28.3±2.5	124.2±34.3	181.1±48.3	ND
% max	73.7±2.9	63.7±3.5	72.2±1.1	54.1±1.5	58.9±2.9	36.0±1.6
(μM; *n*)	(500; 16)	(300; 11)	(300; 7)	(300; 6)	(1000; 5)	(1000; 4)
n_H	1.02±0.05	0.89±0.09	0.94±0.06	0.97±0.07	0.87±0.03	0.87±0.07

Mean ± SEM concentrations of antidepressants (μM) that produce 50% of the maximal effect (EC_{50}) and are required to reduce basal GIRK currents by 25% and 50% (IC_{25} and IC_{50}, respectively) are shown. The % max values indicate the mean ± SEM percentage inhibition of basal GIRK currents by a drug at the highest concentrations tested. The highest concentrations tested (μM) and the number of oocytes tested (*n*) are shown in parentheses. The n_H values indicate the mean ± SEM of Hill coefficients. ND indicates that the value was not determined because of a low effectiveness of the drug.
doi:10.1371/journal.pone.0028208.t001

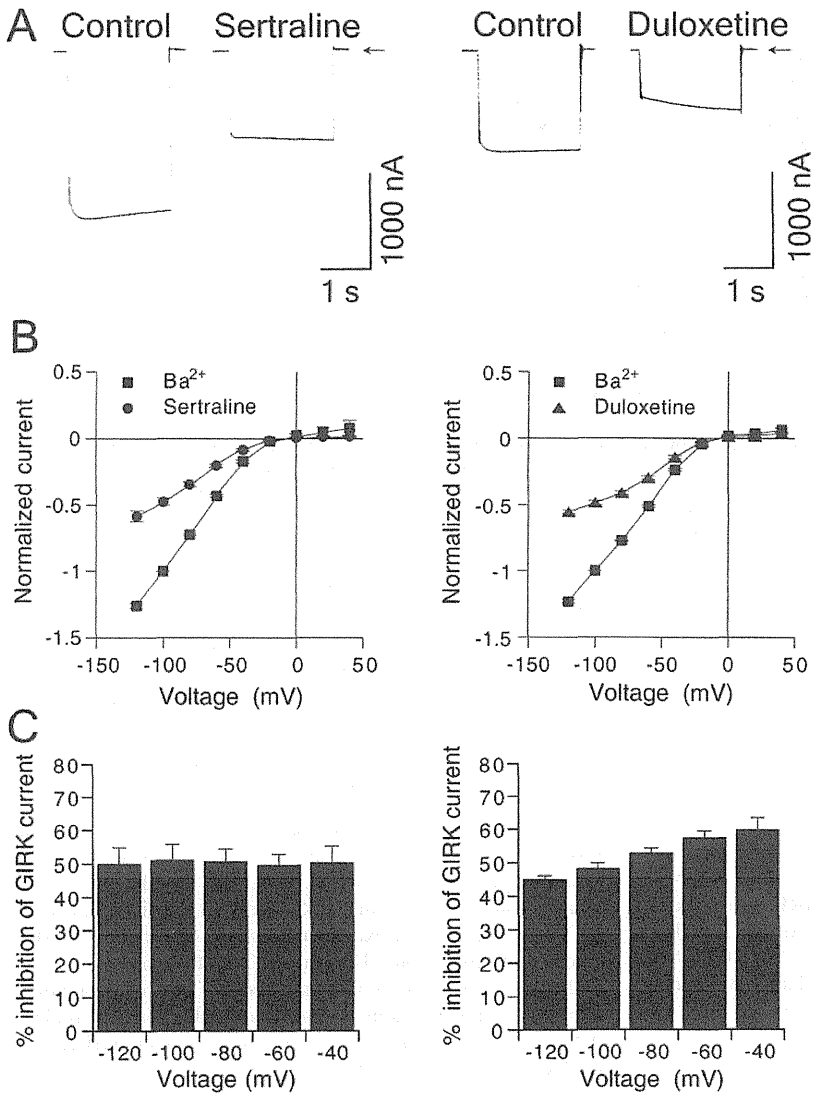

Figure 3. Characteristics of the inhibitory effects of sertraline and duloxetine on GIRK currents. (A) Representative GIRK1/2 currents elicited by a voltage step to −100 mV for 2 s from a holding potential of 0 mV in the presence or absence of 30 μM sertraline (left) or 30 μM duloxetine (right) applied for 3 min. Current responses were recorded in an hK solution that contained 96 mM K^+. Arrows indicate the zero current level. (B) Current-voltage relationships of the magnitudes of 3 mM Ba^{2+}-sensitive currents and the magnitudes of currents reduced by 30 μM sertraline (left, $n=9$) or 30 μM duloxetine (right, $n=6$) in oocytes that expressed GIRK1/2 channels. Current responses were normalized to the 3 mM Ba^{2+}-sensitive current component measured at a membrane potential of −100 mV (1851.0±220.4 nA, $n=15$). (C) Percentage inhibition of GIRK1/2 channels by 30 μM sertraline or 30 μM duloxetine over the voltage range of −120 to −40 mV. The magnitudes of inhibition of GIRK currents by 30 μM sertraline (left, $n=9$) and duloxetine (right, $n=6$) at the end of the voltage pulses were compared with the 3 mM Ba^{2+}-sensitive current components. All values are expressed as mean ± SEM.
doi:10.1371/journal.pone.0028208.g003

Eli Lilly and Company). At physiological pH or below, sertraline and duloxetine exist mainly in a protonated form, approximately 96.9% and 98.9% at pH 7.4, respectively, and the proportion of the uncharged form increases with an increase in pH. We examined whether changes in extracellular pH would affect GIRK channel inhibition by sertraline or duloxetine. However, in oocytes that expressed GIRK1/2 channels, the percentage inhibition of GIRK channels by sertraline or duloxetine at the same concentrations was not significantly affected by extracellular pH 7.4 and 9.0 (no significant pH×drug interaction, $P>0.05$, two-way ANOVA; $P>0.05$ at each concentration, Tukey-Kramer *post hoc* test; Fig. 4). The results indicate that a marked increase in the proportion of the uncharged form of sertraline and duloxetine may not significantly affect all of the inhibitory effects on GIRK channels, suggesting that GIRK channel inhibition may be mediated by both forms of the drugs with similar effectiveness. Additionally, the inhibition by the antidepressants was unlikely mediated by nonspecific membrane perturbation induced by the uncharged form.

Effects of sertraline on GIRK channels activated by GTPγS, a nonhydrolyzable GTP

GIRK channels are activated by various $G_{i/o}$-protein-coupled receptors through the direct action of G-protein βγ subunits

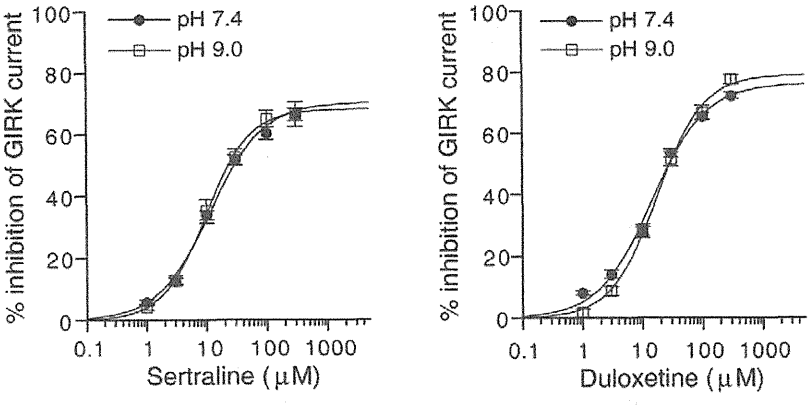

Figure 4. Concentration-dependent inhibition of GIRK channels by sertraline or duloxetine at different pH values. The magnitudes of inhibition of GIRK currents by the antidepressants were compared with the 3 mM Ba^{2+}-sensitive current components in oocytes that expressed GIRK1/2 channels (1020.8±96.2 nA at pH 7.4, $n=16$ for sertraline and $n=7$ for duloxetine; 1079.5±173.8 nA at pH 9.0, $n=7$ for sertraline and $n=6$ for duloxetine, respectively). Current responses were measured at a membrane potential of −70 mV in an hK solution that contained 96 mM K^+. Each point and error bar represent the mean ± SEM of the percentage responses.
doi:10.1371/journal.pone.0028208.g004

released from the heterotrimeric G-protein complex [32,33]. The effects of sertraline on GIRK channels activated by G-protein-coupled signaling mechanisms were further examined using GTPγS, a nonhydrolyzable GTP analog that maintains G-proteins in an activated state. Injection of GTPγS into *Xenopus* oocytes injected with GIRK1 and GIRK2 mRNAs increased inward currents with time and reached a steady-state level (516.0±123.7 nA, $n=5$) as reported previously [49,51]. The increased inward currents were completely blocked by 3 mM Ba^{2+}, whereas GTPγS injection into uninjected oocytes had no significant effect on current responses to 3 mM Ba^{2+} (3.9±2.1 nA, $n=5$). Increased GIRK currents composed of basal GIRK currents and GTPγS-induced GIRK currents were inhibited by sertraline ($IC_{25}=5.5\pm0.7$ μM; $IC_{50}=18.1\pm3.0$ μM; $n_H=1.24\pm0.09$; $n=5$; Fig. 5). The concentration response curve for the inhibition of total GIRK currents by sertraline was partially different from that for the inhibition of basal GIRK currents in GTPγS-untreated oocytes injected with GIRK1 and GIRK2 mRNAs ($P<0.05$ at 30 μM, Tukey-Kramer *post hoc* test, Fig. 5). The results suggest that the potency of the inhibition of GIRK channels activated by GTPγS-induced G-protein activation may be slightly higher than that of basally active GIRK channels, although the maximal efficacy was similar.

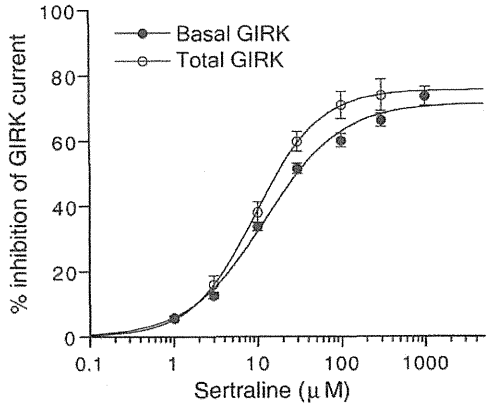

Figure 5. Effects of sertraline on total GIRK currents composed of GTPγS-induced and basal GIRK currents. For comparison, the effects on GTPγS-untreated basal GIRK currents shown in Figure 2 are also shown. The magnitudes of inhibition of GIRK currents by sertraline were compared with the 3 mM Ba^{2+}-sensitive current components. Each point and error bar represent the mean ± SEM of the percentage responses ($n=5$ for GTPγS-injected oocytes and $n=16$ for GTPγS-untreated oocytes). Current responses were measured at a membrane potential of −70 mV in an hK solution that contained 96 mM K^+.
doi:10.1371/journal.pone.0028208.g005

Sertraline inhibits ethanol-induced GIRK currents. GIRK channels are also activated by ethanol independent of G-protein signaling pathways [34]. Sertraline was shown to reduce ethanol consumption in mice [52] and was effective in alcoholics [53]. Therefore, we also examined the effects of sertraline on GIRK channel activation induced by ethanol. The effects of sertraline were evaluated by measuring the amplitude of the ethanol-induced current response during the extracellular application of sertraline at different concentrations. In oocytes injected with GIRK1 and GIRK2 mRNAs, the GIRK currents induced by 100 mM ethanol (344.2±40.3 nA, $n=6$) were reversibly attenuated in the presence of sertraline ($IC_{25}=6.2\pm1.4$ μM; $IC_{50}=29.6\pm5.5$ μM; $n_H=0.87\pm0.17$; $n=6$; Fig. 6A, 6B). However, the 100 mM ethanol-induced GIRK currents were not significantly affected by intracellularly applied sertraline (104.9±9.1% of untreated control current, paired *t*-test, $P>0.1$, $n=6$; Fig. 6C). Moreover, in oocytes that expressed GIRK channels, the basal currents were not substantially affected by intracellularly applied sertraline (92.5±1.6% of untreated control current, $n=6$). The results indicate that intracellular sertraline could not inhibit GIRK channels. In contrast, GIRK channel inhibition induced by extracellularly applied sertraline, which is mainly protonated at pH 7.4, was reversible with washout (Figs. 1A and 6A). Because the protonated form may not readily permeate the cell membrane, extracellularly applied sertraline may exist mainly on the extracellular side. Altogether, extracellular sertraline may inhibit GIRK channels activated by ethanol. Additionally, the extent of inhibition by sertraline of GIRK1/2 channels activated by ethanol was higher at 100 and 300 μM than that of basally active GIRK1/2 channels by G-proteins ($P<0.05$, Tukey-Kramer *post hoc* test), indicating a significant difference in the maximal efficacy of sertraline between ethanol activation of GIRK channels and G-protein activation of the channels.

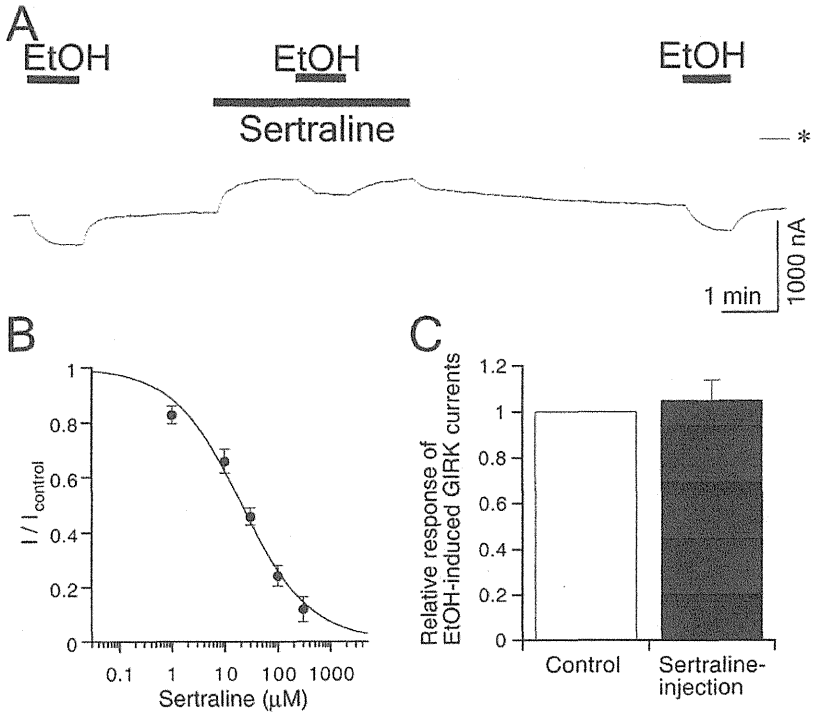

Figure 6. Effect of sertraline on ethanol-induced GIRK currents. (A) Current responses to 100 mM ethanol (EtOH), 100 mM EtOH in the presence of 30 μM sertraline, and 100 mM EtOH in an oocyte injected with GIRK1 and GIRK2 mRNAs. Asterisk indicates the zero current level. Bars show the duration of application. (B) Concentration-dependent inhibition of EtOH-induced GIRK currents by sertraline. $I_{control}$ is the amplitude of GIRK currents induced by 100 mM EtOH (344.2±40.3 nA, $n=6$), and I is the current amplitude in the presence of sertraline. (C) Lack of effect of intracellular sertraline on 100 mM EtOH-induced GIRK currents. The amplitude of EtOH-induced GIRK currents after sertraline injection (black bar) was compared with EtOH-induced GIRK currents before the injection (control, white bar) in the same oocyte that expressed GIRK channels ($n=5$). Current responses were measured at a membrane potential of −70 mV in an hK solution that contained 96 mM K^+. All values are expressed as mean ± SEM.
doi:10.1371/journal.pone.0028208.g006

Discussion

The present study demonstrated that the SSRI sertraline, SNRI duloxetine, and second-generation TCA amoxapine effectively inhibited brain-type GIRK1/2 channels and cardiac-type GIRK1/4 channels expressed in *Xenopus* oocytes. However, the 5-HT_2 receptor antagonist nefazodone, SNRI venlafaxine, and NaSSAs mianserin and mirtazapine weakly inhibited both types of GIRK channels even at high concentrations. The inhibitions by different classes of antidepressants were concentration-dependent with various degrees of potency and effectiveness. In contrast, Kir2.1 channels in other Kir channel subfamilies were insensitive to all of the drugs. Furthermore, the present results suggest that sertraline and duloxetine primarily inhibited GIRK channels at the holding potential of 0 mV before the voltage pulses. The effects of sertraline on GIRK channels were voltage-independent and time-independent during each voltage pulse, similar to the effects of various TCAs [42]. The effects of duloxetine decreased voltage-dependently with negative membrane potentials and time-dependently up to a steady current level in each voltage pulse, and the voltage-dependency was associated with a time-dependent decrease in the inhibition by duloxetine at more negative membrane potentials. The present results also suggest that the site of action on the channels may be extracellular. In contrast, blockade of GIRK channels by extracellular Ba^{2+} and Cs^+, which occlude the pore of the open channel, increases concentration-dependently, voltage-dependently with negative membrane potentials, and time-dependently with a comparatively small effect on the instantaneous current but marked inhibition on the steady-state current at the end of the voltage pulses [27]. These observations suggest that sertraline and duloxetine may cause an allosteric conformational change in GIRK channels, rather than simple occlusion of the open channel. Additionally, sertraline may stably bind to the channels during the voltage pulses, whereas duloxetine may partially dissociate from the channels in the voltage pulses. The n_H values obtained from the concentration-response relationships for sertraline and duloxetine were almost 1 (Table 1), suggesting an one-to-one interaction between the drug and the binding site. Interestingly, GIRK channels were significantly inhibited by the SSRI sertraline and SNRI duloxetine, despite a great difference in the pharmacological profiles for monoamine transporters. The chemical structure of sertraline is distinct from that of duloxetine [2,54]. These antidepressants may act at different binding sites on the channels, and agents with similar structures may interact with GIRK channels. However, the SNRIs venlafaxine and milnacipran [43] had weak or little effects on GIRK channels, respectively. The distinctive effects of the SNRIs on GIRK channels may be attribute to their diverse chemical structures [54]. The *Xenopus* oocyte expression system is useful to determine drug actions on membrane proteins, such as voltage-gated Na^+ and Ca^{2+} channels, glutamate receptor channels, $5HT_{1C}$ receptor [55]. Since neuronal and cardiac GIRK channels are considered to consist predominantly of GIRK1/2 channels and GIRK1/4 channels, respectively [26,29,36], the effects of antidepressants on GIRK1/2 and

GIRK1/4 channels expressed in *Xenopus* oocytes were investigated in the present study. However, GIRK subunits have been suggested to form functional GIRK channels composed of several types of tetrameric stoichimetries in various cell populations, particularly neurons [56]. GIRK1 subunits are posttranslationally modified by glycosylation [26,56,57]. Furthermore, GIRK channels are regulated by not only G proteins but also phosphatidylinositol 4,5-bisphosphate in the cell membrane, polyamines and protein kinases [33]. The effects of antidepressants on GIRK channels might be influenced by differences in composition of the channel subunits, levels of glycosylation of GIRK1 subunits, and interaction with membrane and intracellular factors between the *Xennopus* oocyte expression system and neurons. Further studies using neurons and cardiac myocytes may be useful for advancing our understanding of the effects of antidepressants on GIRK channels.

The therapeutic serum concentrations range from approximately 0.16 to 0.82 μM for sertraline, 0.07 to 0.27 μM for duloxetine, 0.57 to 1.9 μM for amoxapine, 0.02 to 0.64 μM for nefazodone, 0.06 to 0.26 μM for mianserin, 0.08 to 0.37 μM for mirtazapine, and 0.72 to 1.44 μM for venlafaxine [2,58–60]. Additionally, increases in antidepressant doses are associated with increases in blood concentrations [59]. The concentrations in cases of overdose were reported to reach up to 13.7 μM for sertraline [61], 8.4 μM for duloxetine [62], 57.4 μM for amoxapine [63], 11.7 μM for nefazodone, 18.9 μM for mianserin [59], 8.7 μM for mirtazapine [64], and 302.8 μM for venlafaxine [65]. Most of the doses of antidepressants are distributed in various tissues from the blood, and antidepressants generally accumulate in the brain [2,58,66]. Indeed, brain levels of antidepressants were 40-fold higher for sertraline [67], 15-fold higher for duloxetine [68], 8.7- to 35.5-fold higher for amoxapine [69], 1.3- to 1.8-fold higher for nefazodone [70], 12.1-fold higher for mianserin [71], 3.2-fold higher for mirtazapine, and 4.9-fold higher for venlafaxine [66] compared with blood levels. Altogether, due to the high brain-to-blood partition ratios, presumed brain concentrations during treatment with therapeutic doses would range from approximately 6.4 to 32.8 μM for sertraline and 5.0 to 67.5 μM for amoxapine, and those after overdose would reach up to 548 μM for sertraline, 126 μM for duloxetine, 499 or 2038 μM for amoxapine, 229 μM for mianserin, and 1484 μM for venlafaxine. In addition, it has been shown that the therapeutic concentrations of some SSRIs in the brain were much higher than binding affinities of the antidepressants to monoamine transportors [72–75]. Brain concentrations at therapeutic doses of sertraline and amoxapine and after overdose of sertraline, duloxetine, amoxapine, mianserin and venlafaxine overlap with their effective concentrations in inhibiting predominant brain-type GIRK1/2 channels (Fig. 2). Therefore, the present results suggest that some inhibition of GIRK channels in the brain might occur with the antidepressant medication, particularly sertraline. However, mirtazapine and nefazodone may have small or little effects on GIRK channels even at toxic levels. Inhibition of GIRK channels causes a depolarization of membrane potential, resulting in an increase in cell excitability [38]. GIRK channels play an important role in regulating neuronal excitability and synaptic transmission [36,41]. Therefore, even partial inhibition of GIRK channels by the antidepressants may affect various brain functions.

Interestingly, GIRK2 knockout mice exhibit reduced anxiety-related behavior [76]. Animal studies have shown that sertraline has anxiolytic properties [77,78]. Indeed sertraline is clinically effective in the treatment of panic disorder and posttraumatic stress disorder [79]. Although the therapeutic effects are generally thought to be primarily attributable to inhibition of serotonin reuptake in the brain [2], some inhibition of GIRK channels might also contribute to improvement of anxiety symptoms.

Although the risk of seizures with antidepressants is generally very low, the association with overdose is well established [80]. However, the molecular mechanisms by which antidepressants cause seizures have not been clarified. GIRK2 knockout mice exhibit spontaneous seizures and are more susceptible to seizures induced by pentylenetetrazol than wild-type mice [37]. The risk of seizures in overdoses with sertraline, duloxetine, mianserin, and venlafaxine significantly increases [80–82], and amoxapine overdose is more likely to cause seizures [83]. Brain levels of the drugs in overdose cases may be considerably higher than levels during treatment at therapeutic doses, suggesting significant inhibition of neuronal GIRK channels by the drugs. Additionally, other types of K^+ channels are inhibited by antidepressants at micromolar concentrations, that is, the two-pore-domain K^+ channel, TREK-1 for sertraline and voltage-gated K^+ channels for amoxapine and mianserin [16,17,21]. Therefore, the inhibition of GIRK channels by the drugs after overdose together with the different types of K^+ channels may contribute to increased seizure activity and the occurrence of other neurological side effects by increasing neuronal excitability.

In the heart, GIRK channels cause a slowing of heart rate in response to activation of M_2 muscarinic receptors through acetylcholine release from the stimulated vagus nerve [25,26]. GIRK1 and GIRK4 knockout mice exhibit slightly elevated resting heart rates [39]. The present results indicate that sertraline, duloxetine, amoxapine, and venlafaxine can partially inhibit cardiac-type GIRK1/4 channels at blood levels after overdose, although the corresponding heart concentrations were not determined. These antidepressants are associated with sinus tachycardia in cases of toxicity after overdose [81,82,84,85]. In addition, the drugs exhibit low micromolar binding affinities for the muscarinic receptor, with the exception of venlafaxine [2,86], and nanomolar to low micromolar binding affinities for norepinephrine transporters [2,68]. Altogether, sinus tachycardia associated with drug overdose may be related to partial inhibition of atrial GIRK channels as well as antagonism of the muscarinic receptor and enhancement of sympathetic nerve activity.

Sertraline was shown to be effective in the treatment of alcoholics [53]. Interestingly, GIRK2 knockout mice show reduced ethanol-induced conditioned taste aversion and conditioned place preference and are less sensitive than wild-types to some of the acute effects of ethanol, including anxiolysis, habituated locomotor stimulation, and acute handling-induced convulsions [76,87]. In the present study, sertraline inhibited ethanol-induced GIRK1/2 currents. Sertraline may suppress some of the GIRK-related effects of ethanol. Furthermore, GIRK knockout mice show an attenuation of the morphine withdrawal syndrome [88]. Sertraline reduced the severity of the naloxone-precipitated opioid withdrawal syndrome in rats [89]. GIRK knockout mice also show reduced cocaine self-administration [90]. Inhibition of GIRK channels by sertraline may play a role in the treatment of addiction to these drugs.

Supporting Information

Figure S1 Effect of sertraline on outward GIRK currents. In a *Xenopus* oocyte injected with GIRK1 and GIRK2 mRNAs, current responses to 30 μM sertraline and 3 mM Ba^{2+} at a membrane potential of −10 mV in a K4 solution that contained 4 mM K^+ are shown. Asterisk indicates the zero current level.
(DOC)

Acknowledgments

We are grateful to Dr. Kansaku Baba for his cooperation and Mr. Kazuo Kobayashi (Niigata University) for his assistance. We also thank Dr. Lily Y. Jan (University of California, San Francisco) for generously providing the Kir2.1 cDNA.

Author Contributions

Conceived and designed the experiments: TK. Performed the experiments: TK. Analyzed the data: TK KW KI. Contributed reagents/materials/analysis tools: TK KW KI. Wrote the paper: TK KI.

References

1. Kent JM (2000) SNaRIs, NaSSAs, and NaRIs: new agents for the treatment of depression. Lancet 355: 911–918.
2. Baldessarini RJ (2001) Drugs and the treatment of psychiatric disorders: depression and anxiety disorders. In: Hardman JG, Limbird LE, Gilman AG, eds. Goodman & Gilman's The Pharmacological Basis of Therapeutics. 10th edn. New York: McGraw-Hill. pp 447–483.
3. Mann JJ (2005) The management of depression. N Engl J Med 353: 1819–1834.
4. Ni YG, Miledi R (1997) Blockage of $5HT_{2C}$ serotonin receptors by fluoxetine (Prozac). Proc Natl Acad Sci USA 94: 2036–2040.
5. Fan P (1994) Effects of antidepressants on the inward current mediated by 5-HT_3 receptors in rat nodose ganglion neurones. Br J Pharmacol 112: 741–744.
6. Shytle RD, Silver AA, Lukas RJ, Newman MB, Sheehan DV, et al. (2002) Nicotinic acetylcholine receptors as targets for antidepressants. Mol Psychiatry 7: 525–535.
7. Sernagor E, Kuhn D, Vyklicky L, Jr., Mayer ML (1989) Open channel block of NMDA receptor responses evoked by tricyclic antidepressants. Neuron 2: 1221–1227.
8. Nakazawa K, Inoue K, Ohno Y (1999) Block and unblock by imipramine of cloned and mutated $P2X_2$ receptor/channel expressed in *Xenopus* oocytes. Neurosci Lett 264: 93–96.
9. Ogata N, Yoshii M, Narahashi T (1989) Psychotropic drugs block voltage-gated ion channels in neuroblastoma cells. Brain Res 476: 140–144.
10. Mathie A, Wooltorton JRA, Watkins CS (1998) Voltage-activated potassium channels in mammalian neurons and their block by novel pharmacological agents. Gen Pharmacol 30: 13–24.
11. Pancrazio JJ, Kamatchi GL, Roscoe AK, Lynch C, III (1998) Inhibition of neuronal Na^+ channels by antidepressant drugs. J Pharmacol Exp Ther 284: 208–214.
12. Teschemacher AG, Seward EP, Hancox JC, Witchel HJ (1999) Inhibition of the current of heterologously expressed HERG potassium channels by imipramine and amitriptyline. Br J Pharmacol 128: 479–485.
13. Deák F, Lasztóczi B, Pacher P, Petheö GL, Kecskeméti V, et al. (2000) Inhibition of voltage-gated calcium channels by fluoxetine in rat hippocampal pyramidal cells. Neuropharmacology 39: 1029–1036.
14. Choi BH, Choi J-S, Yoon SH, Rhie D-J, Min DS, et al. (2001) Effects of norfluoxetine, the major metabolite of fluoxetine, on the cloned neuronal potassium channel Kv3.1. Neuropharmacology 41: 443–453.
15. Cuellar-Quintero JL, García DE, Cruzblanca H (2001) The antidepressant imipramine inhibits the M-type K^+ current in rat sympathetic neurons. Neuroreport 12: 2195–2198.
16. Scherer D, von Löwenstern K, Zitron E, Scholz EP, Bloehs R, et al. (2008) Inhibition of cardiac hERG potassium channels by tetracyclic antidepressant mianserin. Naunyn-Schmiedeberg's Arch Pharmacol 378: 73–83.
17. He Y-L, Zhan X-Q, Yang G, Sun J, Mei Y-A (2010) Amoxapine inhibits the delayed rectifier outward K^+ current in mousse cortical neurons via cAMP/protein kinase A pathways. J Pharmacol Exp Ther 332: 437–445.
18. Lee K, McKenna F, Rowe ICM, Ashford MLJ (1997) The effects of neuroleptic and tricyclic compounds on BK_{Ca} channels activity in rat isolated cortical neurones. Br J Pharmacol 121: 1810–1816.
19. Dreixler JC, Bian J-T, Cao Y-J, Roberts MT, Roizen JD, et al. (2000) Block of rat brain recombinant SK channels by tricyclic antidepressants and related compounds. Eur J Pharmacol 401: 1–7.
20. Terstappen GC, Pula G, Carignani C, Chen MX, Roncarati R (2001) Pharmacological characterisation of the human small conductance calcium-activated potassium channel hSK3 reveals sensitivity to tricyclic antidepressants and antipsychotic phenothiazines. Neuropharmacology 40: 772–783.
21. Heurteaux C, Lucas G, Guy N, Yacoubi ME, Thümmler S, et al. (2006) Deletion of the background potassium channel TREK-1 results in a depression-resistant phenotype. Nat Neurosci 9: 1134–1141.
22. Maertens C, Droogmans G, Verbesselt R, Nilius B (2002) Block of volume-regulated anion channels by selective serotonin reuptake inhibitors. Naunyn-Schmiedeberg's Arch Pharmacol 366: 158–165.
23. Maertens C, Wei L, Voets T, Droogmans G, Nilius B (1999) Block by fluoxetine of volume-regulated anion channels. Br J Pharmacol 126: 508–514.
24. Reimann F, Ashcroft FM (1999) Inwardly rectifying potassium channels. Curr Opin Cell Biol 11: 503–508.
25. Kubo Y, Reuveny E, Slesinger PA, Jan YN, Jan LY (1993) Primary structure and functional expression of a rat G-protein-coupled muscarinic potassium channel. Nature 364: 802–806.
26. Krapivinsky G, Gordon EA, Wickman K, Velimirovic B, Krapivinsky L, et al. (1995) The G-protein-gated atrial K^+ channel I_{KACh} is a heteromultimer of two inwardly rectifying K^+-channel proteins. Nature 374: 135–141.
27. Lesage F, Guillemare E, Fink M, Duprat F, Heurteaux C, et al. (1995) Molecular properties of neuronal G-protein-activated inwardly rectifying K^+ channels. J Biol Chem 270: 28660–28667.
28. Karschin C, Dißmann E, Stuhmer W, Karschin A (1996) IRK(1–3) and GIRK(1–4) inwardly rectifying K^+ channel mRNAs are differentially expressed in the adult rat brain. J Neurosci 16: 3559–3570.
29. Liao YJ, Jan YN, Jan LY (1996) Heteromultimerization of G-protein-gated inwardly rectifying K^+ channel proteins GIRK1 and GIRK2 and their altered expression in *weaver* brain. J Neurosci 16: 7137–7150.
30. Inanobe A, Yoshimoto Y, Horio Y, Morishige K-I, Hibino H, et al. (1999) Characterization of G-protein-gated K^+ channels composed of Kir3.2 subunits in dopaminergic neurons of the substantia nigra. J Neurosci 19: 1006–1017.
31. North RA (1989) Drug receptors and the inhibition of nerve cells. Br J Pharmacol 98: 13–28.
32. Dascal N (1997) Signalling via the G protein-activated K^+ channels. Cell Signal 9: 551–573.
33. Kobayashi T, Ikeda K (2006) G protein-activated inwardly rectifying potassium channels as potential therapeutic targets. Curr Pharm Des 12: 4513–4523.
34. Kobayashi T, Ikeda K, Kojima H, Niki H, Yano R, et al. (1999) Ethanol opens G-protein-activated inwardly rectifying K^+ channels. Nat Neurosci 2: 1091–1097.
35. Lewohl JM, Wilson WR, Mayfield RD, Brozowski SJ, Morrisett RA, et al. (1999) G-protein-coupled inwardly rectifying potassium channels are targets of alcohol action. Nat Neurosci 2: 1084–1090.
36. Lüscher C, Jan LY, Stoffel M, Malenka RC, Nicoll RA (1997) G protein-coupled inwardly rectifying K^+ channels (GIRKs) mediate postsynaptic but not presynaptic transmitter actions in hippocampal neurons. Neuron 19: 687–695.
37. Signorini S, Liao YJ, Duncan SA, Jan LY, Stoffel M (1997) Normal cerebellar development but susceptibility to seizures in mice lacking G protein-coupled, inwardly rectifying K^+ channel GIRK2. Proc Natl Acad Sci USA 94: 923–927.
38. Kuzhikandathil EV, Oxford GS (2002) Classic D1 dopamine receptor antagonist *R*-(+)-7-chloro-8-hydroxy-3-methyl-1-phenyl-2,3,4,5-tetrahydro-1*H*-3-benzazepine hydrochloride (SCH23390) directly inhibits G protein-coupled inwardly rectifying potassium channels. Mol Pharmacol 62: 119–126.
39. Bettahi I, Marker CL, Roman MI, Wickman K (2002) Contribution of the Kir3.1 subunit to the muscarinic-gated atrial potassium channel I_{KACh}. J Biol Chem 277: 48282–48288.
40. Hashimoto N, Yamashita T, Tsuruzoe N (2006) Tertiapin, a selective IK_{ACh} blocker, terminates atrial fibrillation with selective atrial effective refractory period prolongation. Pharmacol Res 54: 136–141.
41. Lüscher C, Slesinger PA (2010) Emerging roles for G protein-gated inwardly rectifying potassium (GIRK) channels in health and disease. Nat Rev Neurosci 11: 301–315.
42. Kobayashi T, Washiyama K, Ikeda K (2004) Inhibition of G protein-activated inwardly rectifying K^+ channels by various antidepressant drugs. Neuropsychopharmacology 29: 1841–1851.
43. Kobayashi T, Washiyama K, Ikeda K (2006) Inhibition of G protein-activated inwardly rectifying K^+ channels by the antidepressant paroxetine. J Pharmacol Sci 102: 278–287.
44. Kobayashi T, Ikeda K, Ichikawa T, Abe S, Togashi S, et al. (1995) Molecular cloning of a mouse G-protein-activated K^+ channel (mGIRK1) and distinct distributions of three GIRK (GIRK1, 2 and 3) mRNAs in mouse brain. Biochem Biophys Res Commun 208: 1166–1173.
45. Kobayashi T, Ikeda K, Kumanishi T (2000) Inhibition by various antipsychotic drugs of the G-protein-activated inwardly rectifying K^+ (GIRK) channels expressed in *Xenopus* oocytes. Br J Pharmacol 129: 1716–1722.
46. Kubo Y, Baldwin TJ, Jan YN, Jan LY (1993) Primary structure and functional expression of a mouse inward rectifier potassium channel. Nature 362: 127–133.
47. Kobayashi T, Ikeda K, Kumanishi T (2002) Functional characterization of an endogenous *Xenopus* oocyte adenosine receptor. Br J Pharmacol 135: 313–322.
48. Ikeda K, Yoshii M, Sora I, Kobayashi T (2003) Opioid receptor coupling to GIRK channels: in vitro studies using a Xenopus oocyte expression system and in vivo studies on weaver mutant mice. Methods Mol Med 84: 53–64.
49. Kovoor A, Henry DJ, Chavkin C (1995) Agonist-induced desensitization of the mu opioid receptor-coupled potassium channel (GIRK1). J Biol Chem 270: 589–595.
50. Kobayashi T, Washiyama K, Ikeda K (2003) Inhibition of G protein-activated inwardly rectifying K^+ channels by fluoxetine (Prozac). Br J Pharmacol 138: 1119–1128.
51. Kobayashi T, Washiyama K, Ikeda K (2010) Inhibition of G-protein-activated inwardly rectifying K^+ channels by the selective norepinephrine reuptake inhibitors atomoxetine and reboxetine. Neuropsychopharmacology 35: 1560–1569.

52. Gulley JM, McNamara C, Barbera TJ, Ritz MC, George FR (1995) Selective serotonin reuptake inhibitors: effects of chronic treatment on ethanol-reinforced behavior in mice. Alcohol 12: 177–181.
53. Pettinati HM, Volpicelli JR, Kranzler HR, Luck G, Rukstalis MR, et al. (2000) Sertraline treatment for alcohol dependence: interactive effects of medication and alcoholic subtype. Alcohol Clin Exp Res 24: 1041–1049.
54. Stahl SM, Grady MM, Moret C, Briley M (2005) SNRIs: their pharmacology, clinical efficacy, and tolerability in comparison with other classes of antidepressants. CNS Spectr 10: 732–747.
55. Sigel E (1990) Use of *Xenopus* oocytes for the functional expression of plasma membrane proteins. J Membrane Biol 117: 201–221.
56. Aguado C, Colón J, Ciruela F, Schlaudraff F, Cabanero MJ, et al. (2008) Cell type-specific subunit composition of G protein-gated potassium channels in the cerebellum. J Neurochem 105: 497–511.
57. Pabon A, Chan KW, Sui JL, Wu X, Logothetis DE, et al. (2000) Glycosylation of GIRK1 at Asn^{119} and ROMK1 at Asn^{117} has different consequences in potassium channel function. J Biol Chem 275: 30677–30682.
58. Musshoff F, Padosch S, Steinborn S, Maeda SSB (2004) Fatal blood and tissue concentrations of more than 200 drugs. Forensic Sci Int 142: 161–210.
59. Welzen M, Uges DRA (2004) TIAFT reference blood level list of the therapeutic and toxic substances. http://www.tiaft.org.
60. Lobo ED, Bergstrom RF, Reddy S, Quinlan T (2008) In vitro and in vivo evaluations of cytochrome P450 1A2 interactions with duloxetine. Clin Pharmacokinet 47: 191–202.
61. Goeringer KE, Raymon L, Christian GD, Logan BK (2000) Postmortem forensic toxicology of selective serotonin reuptake inhibitors: a review of pharmacology and report of 168 cases. J Forensic Sci 45: 633–648.
62. Vey EL, Kovelman I (2010) Adverse events, toxicity and post-mortem data on duloxetine: case reports and literature survey. J Forensic Legal Med 17: 175–185.
63. Taylor RL, Crooks CR, Caplan YH (1982) The determination of amoxapine in human fatal overdoses. J Anal Toxicol 6: 309–311.
64. Holzbach R, Jahn H, Pajonk FG, Mähne C (1998) Suicide attempts with mirtazapine overdose without complications. Biol Psychiatry 44: 925–926.
65. Levine B, Jenkins AJ, Queen M, Jufer R, Sialek JE (1996) Distribution of venlafaxine in three postmortem cases. J Anal Toxicol 20: 502–505.
66. Uhr M, Grauer MT, Holsboer F (2003) Differential enhancement of antidepressant penetration into the brain in mice with abcb1ab (mdr1ab) P-glycoprotein gene distruption. Biol Psychiatry 54: 840–846.
67. Tremaine LM, Welch WM, Ronfeld RA (1989) Metabolism and disposition of the 5-hydroxytriptamine uptake blocker sertraline in the rat and dog. Drug Metab Dispos 17: 542–550.
68. Bymaster FP, Lee TC, Knadler MP, Detke MJ, Iyengar S (2005) The dual transporter inhibitor duloxetine: a review of its preclinical pharmacology, pharmacokinetic profile, and clinical results in depression. Curr Pharm Des 11: 1475–1493.
69. Sedgwick P, Spiehler VR, Lowe DR (1982) Toxicological findings in amoxapine overdose. J Anal Toxicol 6: 82–84.
70. Nacca A, Guiso G, Fracasso C, Cervo L, Caccia S (1996) Brain-to-blood partition and *in vivo* inhibition 5-hydroxytryptamine reuptake and quipazine-mediated behaviour of nefazodone and its main active metabolites in rodents. Br J Pharmacol 125: 1617–1623.
71. Altamura AC, De Novelis F, Mauri MC, Gomeni R (1987) Plasma and brain pharmacokinetics of mianserin after single and multiple dosing in mice. Prog Neuropsychopharmacol Biol Psychiatry 11: 23–33.
72. Karson CN, Newton JEO, Livingston R, Jolly JB, Cooper TB, et al. (1993) Human brain fluoxetine concentrations. J Neuropsychiatry Clin Neurosci 5: 322–329.
73. Bolo NR, Hode Y, Nedelec J-F, Laine E, Wagner G, et al. (2000) Brain pharmacokinetics and tissue distribution *in vivo* of fluvoxamine and fluoxetine by fluorine magnetic resonance spectroscopy. Neuropsychopharmacology 23: 428–438.
74. Henry ME, Moore CM, Kaufman MJ, Michelson D, Schmidt ME, et al. (2000) Brain kinetics of paroxetine and fluoxetine on the third day of placebo substitution: a fluorine MRS study. Am J Psychiatry 157: 1506–1508.
75. Henry ME, Schmidt ME, Hennen J, Villafuerte RA, Butman ML, et al. (2005) A comparison of brain and serum pharmacokinetics of *R*-fluoxetine and racemic fluoxetine: a 19-F MRS study. Neuropsychopharmacology 30: 1576–1583.
76. Blednov YA, Stoffel M, Chang SR, Harris RA (2001) Potassium channels as targets for ethanol: studies of G-protein-coupled inwardly rectifying potassium channel 2 (GIRK2) null mutant mice. J Pharmacol Exp Ther 298: 521–530.
77. Sánchez C, Meier E (1997) Behavioral profiles of SSRIs in animal models of depression, anxiety and aggression. Psychopharrmacology 129: 197–205.
78. Harada Y, Kohara N, Imaeda T (2006) Pharmacological, pharmacokinetic, and clinical profile of sertraline hydrochloride (J ZOLOFT™). Folia Pharmacol Jpn 128: 417–424.
79. Schatzberg AF (2000) New indications for antidepressants. J Clin Psychiatry 61(Suppl 11): 9–17.
80. Montgomery SA (2005) Antidepressants and seizures: emphasis on newer agents and clinical implications. Int J Clin Pract 59: 1435–1440.
81. Whyte IM, Dawson AH, Buckley NA (2003) Relative toxicity of venlafaxine and selective serotonin reuptake inhibitors in overdose compared to tricyclic antidepressants. Q J Med 96: 369–374.
82. Isbister GK, Bowe SJ, Dawson A, Whyte IM (2004) Relative toxicity of selective serotonin reuptake inhibitors (SSRIs) in overdose. J Toxicol Clin Toxicol 42: 277–285.
83. Litovitz TL, Troutman WG (1983) Amoxapine overdose: seizures and fatalities. JAMA 250: 1069–1071.
84. Frommer DA, Kulig KW, Marx JA, Rumack B (1987) Tricyclic antidepressant overdose: a review. JAMA 257: 521–526.
85. Lott RS, Baker DE (2003) Duloxetine: a new antidepressant. Advances Pharmacy 1: 228–241.
86. Bymaster FP, Dreshfield-Ahmad LJ, Threlkeld PG, Shaw JL, Thompson L, et al. (2001) Comparative affinity of duloxetine and venlafaxine for serotonin and norepinephrine transporters in vitro and in vivo, human serotonin receptor subtypes, and other neuronal receptors. Neuropsychopharmacology 25: 871–880.
87. Hill KG, Alva H, Blednov YA, Cunningham CL (2003) Reduced ethanol-induced conditioned taste aversion and conditioned place preference in GIRK2 null mutant mice. Psychopharmacology 169: 108–114.
88. Cruz HG, Berton F, Sollini M, Blanchet C, Pravetoni M, et al. (2008) Absence and rescue of morphine withdrawal in KIR/Kir3 knock-out mice. J Neurosci 28: 4069–4077.
89. Gray AM (2002) The effect of fluvoxamine and sertraline on the opioid withdrawal syndrome: a combined in vivo cerebral microdialysis and behavioural study. Eur Neuropschopharmacol 12: 245–254.
90. Morgan AD, Carroll ME, Loth AK, Stoffel M, Wickman K (2003) Decreased cocaine self-administration in Kir3 potassium channel subunit knockout mice. Neuropsychopharmacology 28: 932–938.

Pharmacogenomics of the human μ-opioid receptor

The μ-opioid receptor is a primary target for clinically important opioid analgesics, including morphine, fentanyl and methadone. Many genetic variations have been identified in the human μ-opioid receptor MOP gene (*OPRM1*), and their implications have been reported in the effects of opioid drugs and susceptibility to drug dependence. Interestingly, agonistic and antagonistic opioid effects are inversely associated with the A118G polymorphism genotype. The A118G polymorphism may also be associated with substance dependence and susceptibility to other disorders, including epilepsy and schizophrenia. The IVS1+A21573G, IVS1-T17286C, and TAA+A5359G polymorphisms in the *OPRM1* gene may be associated with alcohol, opioid and tobacco dependence, respectively. However, some studies have failed to confirm the correlations between the polymorphisms and opioid effects and substance dependence. Further studies are needed to elucidate the molecular mechanisms underlying the effects of *OPRM1* polymorphisms.

KEYWORDS: μ-opioid receptor analgesia drug addiction genetic polymorphism narcotic drugs

Shinya Kasai[1] & Kazutaka Ikeda[1]

[1]Research Project for Addictive Substances, Tokyo Metropolitan Institute of Medical Science, 2-1-6 Kamikitazawa, Setagaya-ku, Tokyo 156-8506, Japan
*Author for correspondence:
Tel.: +81 368 342 390
Fax: +81 368 342 390
kasai-syi@igakuken.or.jp

Pharmacological importance of the μ-opioid receptor

The μ-opioid receptor (MOP) is a subtype that belongs to the superfamily of 7-transmembrane-spanning G-protein-coupled receptors. Pharmacological studies with gene-knockout mice show that MOP is a major target for the clinically important opioid drugs, such as morphine and fentanyl, and it appears to play critical roles in the mediation of the major effects of these opioid drugs, including analgesia, tolerance, dependence and respiratory depression [1,2,20]. Homozygous MOP-deficient mice are insensitive to morphine [3–5]. In addition, heterozygous MOP-deficient mice, which possess approximately half of the amount of MOP protein in wild-type mice, exhibit haploinsufficiency in the analgesic effects of morphine [4,5]. The CXBK mouse strain, a recombinant inbred strain derived from an F2 intercross between BALB/c and C57BL/6 mice, exhibit reduced responses to opioid receptor agonists [6]. The CXBK strain expresses approximately half of the amount of MOP mRNA compared with progenitor strains and display phenotypes similar to those of heterozygous MOP-deficient mice [7]. In the CXBK strain, an intracisternal A-particle transposon is inserted in the 3′-UTR of the MOP gene, which would be expected to be the cause of the reduced response to opioids [8]. Among wild-derived inbred mouse strains, many genetic variations were identified in the mouse MOP gene, and some of these variations were associated with interstrain differences in opioid sensitivity [9]. These results suggest that genetic variations in the MOP gene and MOP expression influence morphine sensitivity in a gene dosage-dependent manner.

In this brief article, we focus on and summarize the genetic variations in the human MOP gene, which are analyzed with regard to pain sensitivity, opioid drug sensitivity and susceptibility to drug dependence, and other disorders.

Structure of the human MOP gene

The cDNAs and genes encoding MOP have been cloned from mouse, rat, porcine, bovine, and human sources [10 • 17]. The human MOP gene (*OPRM1*) spans over 200 kb and consists of 11 exons that combine to yield 17 splice variants [18]. The exons A/B, X, Y and 5A–E in intron 1 or 3 of the *OPRM1* gene yield variants such as MOR-1B1–1B5, MOR-1X, MOR-1Y, SV1 and SV2 (Figure 1). Among the transcripts from the *OPRM1* gene, MOR-1, which consists of exons 1, 2, 3, and 4, is approximately 15 kb in length and the most abundant transcript [19]. The MOR-1 3′-UTR is continuously transcribed, beginning with the exon 4 coding region of MOR-1 mRNA. Human MOR-1 mRNA possesses a long 3′-UTR of over 13 kb. The other variants of the *OPRM1* gene, including MOR-1B5 and MOR-1Y, are also long transcripts defined as 15 kb, but the 3′-UTRs for these variants have not been identified [20].

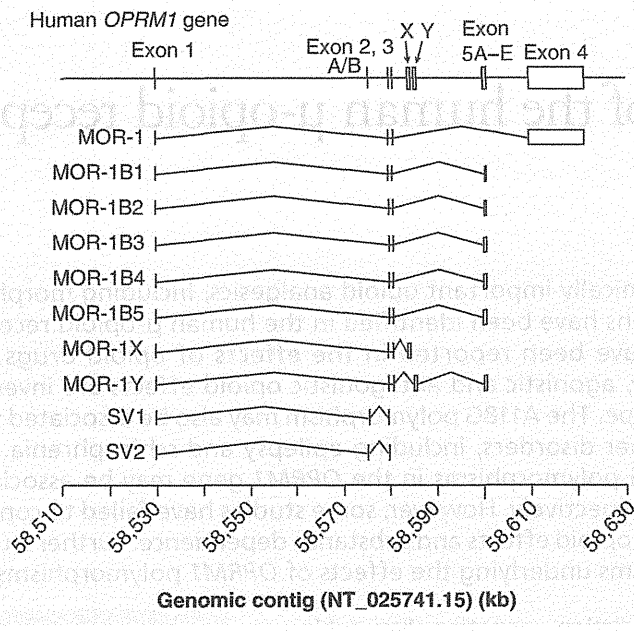

Figure 1. Human μ-opioid receptor gene (*OPRM1*) structure. The human *OPRM1* gene spans over 200 kb and consists of multiple exons that combine to yield isoforms. Among these isoforms, MOR-1, which consists of exons 1, 2, 3 and 4 of the *OPRM1* gene, is approximately 15 kb in length and is the most abundant transcript. Exon A/B was identified in intron 1 as the first exon for the splice variants SV1 and SV2. In intron 3, exons X, Y and 5 were also identified as the last exons for the variants MOR-1X, MOR-1Y and MOR-1B1–1B5, respectively.

The human MOP gene structure and splicing sites are similar to those of mice [19,21]. Mouse MOR-1 mRNA is transcribed from exons 1, 2, 3 and 4 and possesses a long 3′-UTR of over 10 kb, which is continuously transcribed from exon 4, similar to human MOR-1 mRNA. Human MOR-1 (GenBank accession no. L25119) shares 87% cDNA and 94% amino acid sequence identities with mouse MOR-1 (GenBank accession no. U19380) [202]. The 3′-UTR of human MOR-1 mRNA shows high similarity to mouse MOR-1 mRNA in the regions of their 5′ and 3′ ends [19]. Many splice variants of MOR-1 mRNA have also been reported in mice. Studies with antibodies against splice variants of mouse MOR-1 mRNA and gene-modified mice for exon 11 were performed [22–25], but the functions of these splice variants of MOR-1 mRNA have been controversial.

SNPs in the *OPRM1* gene

Over 700 SNPs have been identified in the *OPRM1* gene (refer to the dbSNP database, the NCBI database of genetic variations) [203]. Genetic variations in the *OPRM1* gene are quite different between different races and ethnicities. In the International HapMap project, genetic variations in the African population in Nigeria (YRI), northern and western European ancestry in the USA (CEU), Japanese in Tokyo, Japan (JPT), and Han Chinese in Beijing, China (CHB) were analyzed, and variations in the SNPs in the *OPRM1* gene were the following: CEU > YRI > JPT and CHB [204]. These data suggest that the linkage disequilibrium (LD) blocks and minor allele frequencies (MAFs) of the SNPs in the *OPRM1* gene are different between different races and ethnicities.

In European populations (European Americans or Caucasians), the *OPRM1* gene is covered with two LD blocks whose boundary is located around the end of intron 1 between rs3778156 and rs2075572, rs1381376 and rs9479757, rs1381376 and rs563649, or rs3778151 and rs660756 [26–30]. In American Indians, the *OPRM1* gene also consists of two major LD blocks that are separated by the border between rs506247 and rs2075572 [31]. However, in the Japanese population, the *OPRM1* gene is covered with four LD blocks [32]. In the Uyghur population, the major LD blocks were not identified in the *OPRM1* gene, but a small LD block was identified at intron 3 containing rs3798683 and rs9397685 [33]. The MAFs of A118G (rs1799971), which is a well-studied nonsynonymous SNP leading to an Asn40Asp substitution in the *OPRM1* gene, are 0.047 in the African population, 0.154 in the European population, 0.485 in the Japanese population, 0.14 in the Hispanic population, 0.210 in the Ashkenazi population, 0.08 in the Bedouin population and 0.17 in the Ethiopian population, indicating a wide variety of MAFs of the A118G SNP in the *OPRM1* gene among different races and ethnicities [34]. These results suggest that genetic variations in the *OPRM1* gene need to be analyzed by the race/ethnicity of populations.

Numerous SNPs in the *OPRM1* gene have been analyzed with regard to clinical traits (Supplementary Table 1; www.futuremedicine.com/doi/suppl/10.2217/pgs.11.68). Supplementary Table 1 lists the SNPs in the *OPRM1* gene that were previously reported in association studies, with the exception of haplotype analyses, pain sensitivity, opioid sensitivity, and susceptibility to drug dependence and other disorders. Almost all of the analyzed SNPs in the *OPRM1* gene are located at exons 1–4, corresponding to the genomic region for the MOR-1 mRNA.

Association studies of SNPs in the *OPRM1* gene & pain sensitivity

Homozygous and heterozygous MOP-deficient mice exhibited higher sensitivity to thermal nociception compared with wild-type mice

in the tail-flick test at 50°C and 53°C [4]. These data suggest that hypomorphic SNPs in *OPRM1*, which reduce their expression or function, influence pain sensitivity.

Four SNPs in the *OPRM1* gene were analyzed in association studies with pain and related traits (TABLE 1) [35–43]. Among four SNPs, the IVS1-C2994T and IVS2+G31A SNPs were significantly associated with pain sensitivity scores and pressure pain thresholds, respectively [35,43]. However, no other reports have shown an association between these two SNPs and pain-related traits; therefore, the results of these association studies remain controversial. Significant associations with pain-related traits were also observed in studies of the A118G SNP. The G-allele carriers of the A118G SNP showed higher reactivity to social rejection compared with AA subjects in the dorsal anterior cingulate cortex and anterior insula, which are involved in processing social and physical pain [41]. However, G-allele carriers exhibited lower sensitivity to mechanical stimulation than AA subjects did [36]. Therefore, Further studies are necessary to evaluate the results of these association studies between the A118G SNP and pain sensitivity.

Association of *OPRM1* SNPs with opioid sensitivity

The MOP plays an integral role in the various effects of opioids. Morphine, fentanyl and methadone are agonists for the MOP, and the clinical effects of these analgesic opioids, such as analgesia and their side effects, including nausea, vomiting, pruritis and respiratory depression, are mainly produced through MOP [2]. The analgesic and side effects of analgesic opioids were abolished or reduced in homozygous or heterozygous MOP-deficient mice [4,5]. These results indicate that MOP gene dosage is related to the clinical efficacy of analgesic opioids. In addition, the opioid antagonist naltrexone is effective for the treatment of alcohol dependence [44]. Naltrexone is a nonspecific antagonist of opioid receptor subtypes, but it strongly interacts with MOP [45]. The effects of naltrexone on drinking outcome have been found to be greater in alcoholic individuals with a family history of alcoholism [46,47], suggesting that genetic factors highly contribute to the effects of naltrexone in alcoholic treatment. Furthermore, the endogenous opioidergic system via MOP plays a critical role in the regulation of hypothalamic–pituitary–adrenal (HPA) axis activation. Corticotropin-releasing factor neurons in the paraventricular nucleus of the hypothalamus, which expresses MOP, initiates HPA axis activation [48,49]. Opioid blockade by naloxone has been found to show a greater cortisol response among individuals with a family history of alcoholism [50–52]. Thus, genetic variations in the *OPRM1* gene appear to affect the analgesic and side effects of opioids, efficacy of naltrexone for alcoholic treatment, and HPA axis activation by naloxone and exhibit interindividual differences in these effects of opioids.

Many SNPs in the *OPRM1* gene have been investigated in regard to opioid sensitivity, including the analgesic and side effects of analgesic opioids, efficacy of naltrexone for alcoholic treatment, and HPA axis activation by naloxone (TABLE 2) [37,40,42,53–96]. Among these studies, statistical significance was found in association studies between only three SNPs (A118G, IVS2+C691G and IVS3+A8449G) and opioid sensitivity.

The A118G SNP has been shown to be associated with the analgesic and side effects of opioids, including morphine, morphine-6-glucuronide (M6G) and fentanyl. In these studies, opioid dose [66,76], consumption [42,68], requirement [54,56,63,64,80], and 50% effective concentration (EC_{50}) [58,62] were greater in G-allele carriers compared with AA subjects, regardless of the analgesic and analgesia type. Specifically, the analgesic effects were lower in

Table 1. Association studies of *OPRM1* SNPs with pain sensitivity.

Polymorphism	Result (MAF)	Ref.
G-172T	No (pressure pain threshold and tolerance) (0.174)	[35]
C17T	Not analyzed (0.000)	[35]
A118G	No (heat pain threshold) (0.112)	[36]
	G-allele carriers > AA subjects (pressure pain threshold, $p < 0.05$)	
	No (ischemic pain threshold)	
	No (MPQ-sensory postoperative pain rating) (0.125)	[37]
	Association (MPQ-sensory and MPQ-affective pain ratings, $p < 0.05$)	[38]
	No (pressure pain threshold and tolerance) (0.319)	[35]
	No (chronic widespread pain) (0.100)†	[39]
	No (cold pressor-induced pain threshold) (0.438)	[40]
	G-allele carriers > AA subjects (dispositional and neural sensitivity, $p < 0.05$) (0.208)	[41]
	G-allele carriers < AA patients (pain tolerance threshold, $p = 0.03$ and 0.001) (0.313)	[42]
IVS1-C2994T	Association (pain-sensitivity score, $p = 0.0007$)	[43]
	No (chronic widespread pain) (0.093)†	[39]
IVS2+G31A	GA subjects > GG subjects (pressure pain threshold, $p = 0.036$) (0.028)	[35]
	No (pressure pain tolerance)	
IVS2+C691G	Not analyzed (0.000)	[35]

†The number of subjects combined the control and chronic widespread pain groups.
MAF: Minor allele frequency; MPQ: McGill Pain Questionnaire.

G-allele carriers than in AA subjects. G-allele carriers exhibited lower analgesic efficacy compared with AA subjects [40,67,70,73,75]. Similar to analgesic efficacy, the incidence of analgesic opioid side effects was lower in G-allele carriers than in AA subjects [56,60,68,73,75,77]. Numerous studies have also reported associations of the A118G SNP with the efficacy of naltrexone for alcoholic treatment. In contrast to the effects of analgesic opioids, the efficacy of naltrexone for alcoholic treatment (i.e., rate of relapse, time to relapse, craving for alcohol and clinical outcome) were higher in G-allele carriers than AA patients [57,84,86,88,89]. Similarly, HPA axis activation induced by naloxone was greater in G-allele carriers than AA subjects [93–96]. These results indicate that the G allele of the A118G SNP is hypomorphic and hypermorphic for the effects of analgesic opioids and opioid antagonists, respectively. The meta-analysis showed an association of the A118G SNP with less nausea (effect size, Cohen's d = -0.21, p = 0.037) and more dosage requirements (d = 0.56, p = 0.018) in GG subjects [97]. However, some reports showed no association between the A118G SNP and opioid sensitivity. Association studies of opioid sensitivity have been performed with various races and population ethnicities. As described above, the MAFs of the A118G SNP vary widely among race/ethnicity; therefore, the effect sizes of the A118G SNP in association studies are quite different between races and ethnicities. A possible explanation for the incidence of no association between the A118G SNP and effects of opioids is that the statistical power was inadequate and may be attributable to the different MAFs between races and ethnicities in the sample populations. The MAF in the studies of the association between the A118G SNP and analgesic effects of opioids is 0.260 ± 0.032 (n = 16, average ± standard error of the mean), which tends to be higher than the MAF in studies that found no association between the A118G SNP and analgesic effects of opioids (0.173 ± 0.067, n = 5). However, the MAFs in the studies that found an association between the A118G SNP and side effects of analgesic opioids or efficacy of naltrexone for alcoholic treatment, are not different from the studies that found no associations. These opioid functions are dependent on metabolic enzymes, transporters and molecules involved in opioid signal transduction pathways. Specifically, the side effects of opioid analgesics are under the influence of drug-metabolizing enzymes and transporters, which facilitate the elimination of opioids from the body (e.g., CYP, UDP-glucuronosyltransferase and ATP-binding cassette transporters). Therefore, genetic variations in the genes that encode these molecules might be involved in opioid sensitivity and affect the association between the A118G SNP in the *OPRM1* gene and the side effects of opioid analgesics. Naltrexone exerts its effect by interacting not only with MOP but also with δ- and κ-opioid receptors. The A118G SNP in the *OPRM1* gene may be associated with the action of opioids, such as morphine and fentanyl, at the MOP rather than affect the action of nonspecific opioids, such as naltrexone, at other opioid receptor subtypes. The reasons as to why some studies did not confirm the association between the A118G SNP and side effects of analgesic opioids or treatment efficacy of naltrexone for alcoholism, remain to be clarified.

In an association study of the IVS2+C691G SNP, statistical significance was observed with the effects of naloxone [96], but another study did not show an association between the IVS2+C691G SNP and analgesic effects of morphine or fentanyl. Similar to the IVS2+C691G SNP, only one study reported an association between the IVS3+A8449G SNP and fentanyl analgesia [40]. Therefore, further work is needed to validate and determine the significance of the IVS2+C691G and IVS3+A8449G SNPs in the effects of naloxone and fentanyl analgesia, respectively.

Association of *OPRM1* SNPs with susceptibility to substance dependence

Pharmacological studies in animals implicate the endogenous opioid system in the reinforcing effects of a variety of drugs, including alcohol, cocaine, heroin, cannabinoids, nicotine and amphetamine. These drugs have been shown to release dopamine in the nucleus accumbens and ventral tegmental area, which are critical brain loci in the reinforcement pathway [98]. Dopamine release is a consequence of increased opioidergic activity, which inhibits GABA neurons, thereby disinhibiting dopaminergic neurons [99]. MOP-deficient mice exhibited decreased ethanol self-administration and decreased ethanol intake [100–102]. The rewarding effects of heroin, cannabinoids and nicotine, but not amphetamine, were also abolished or reduced in MOP-deficient mice [103–108]. Cocaine reward, measured by conditioned place preference, was reduced in both homozygous and heterozygous MOP-deficient mice [109], although cocaine produced comparable conditioned place preference in both wild-type and MOP-deficient mice

Table 2. Association studies of *OPRM1* SNPs with the effects of opioid drugs.

Polymorphism	Opioid	Opioid effect	Result	Number of subjects	Ref.
G-1784A	Morphine	Cancer pain relief	GA carrier < GG carrier (pain relief)	GG, 1; GA, 1; AA, 0	[53]
G-172T	Morphine	Cancer pain relief	No (morphine requirement)	GG, 90; GT, 8; TT, 1	[54]
	Morphine	Cancer pain relief	No (opioid switching)	GG, 137; GT, 19; TT, 0†	[55]
	Morphine	Postoperative analgesia	No (morphine requirement)	GG, 819; GT, 156; TT, 8	[56]
		Side effects	No (nausea, vomiting episodes and pruritis)		
C17T	Naltrexone	Alcoholic treatment	Not analyzed	CC, 6; CT, 5; TT, 0	[57]
A118G	Morphine	Pupil constriction	No (EC_{50} of morphine)	AA, 6; AG, 5; GG, 1	[58]
	Morphine	Morphine tolerance	Morphine tolerance with high plasma M6G in GG subjects	AA, 1; AG, 0; GG, 1	[59]
		Side effects	Dizziness, sleepiness and apathy in AA subjects		
	Morphine/M6G	Pupil constriction	G-allele carriers < AA subjects (miotic effects of morphine and M6G)	AA, 6; AG, 4; GG, 2	[60]
		Side effects	G-allele carriers < AA subjects (nausea and vomiting, $p < 0.05$)		
	Morphine	Cancer pain relief	Less effective in AG patients	AA, 1; AG, 1; GG, 0	[53]
	Morphine	Cancer pain relief	GG patients > AA patients (morphine requirement, $p = 0.006$)	AA, 78; AG, 17; GG, 4	[54]
		Side effects	No (nausea, vomiting, dyspnea, sleepiness, loss of appetite and constipation)		
	Morphine	Cancer pain relief	No (opioid switching)	AA, 114; AG, 37; GG, 5†	[55]
	Morphine	Postoperative analgesia	No (morphine dose)	AA, 57; AG, 15; GG, 2	[61]
		Side effects	No (PONV requiring ondansetron)		
	Morphine/M6G	Pupil constriction	GG subjects > AA subjects (EC_{50} of opioids, $p < 0.001$)	AA, 23; AG, 6; GG, 2	[62]
	Morphine	Cancer pain relief	GG patients > AA patients (morphine requirement, $p = 0.024$)	AA, 43; AG, 19; GG, 18	[63]
		Side effects	No (nausea score, vomiting and sedation score)		
	Morphine	Postoperative analgesia	GG patients > AA patients (morphine requirement, $p = 0.003$)	AA, 74; AG, 33; GG, 13	[64]
		Side effects	No (nausea, vomiting, and other adverse effects)		
	Morphine/fentanyl	Postoperative analgesia	No (morphine dose)	AA, 70; AG, 30; GG, 1	[65]
	Morphine	Cancer pain relief	G-allele carriers > AA patients (morphine dose, $p = 0.012$)	AA, 166; AG, 36; GG, 5	[66]
	Morphine	Cancer pain relief	GG patients < AA patients (pain relief, $p < 0.001$)	AA, 106; AG, 22; GG, 10	[67]
	Morphine	Postoperative analgesia	G-allele carriers > AA subjects (morphine consumption, $p < 0.05$)	AA, 272; AG, 234; GG, 82	[68]
		Side effects	G-allele carriers < AA subjects (nausea, $p = 0.02$)		
		Side effects	No (pruritus severity score)		
	Morphine	Postoperative analgesia	Association (morphine requirement, $p < 0.01$)	AA, 389; AG, 435; GG, 170	[56]
		Side effects	Association (nausea, $p = 0.026$; vomiting episodes, $p = 0.022$)		

†*The number of subjects combined the control and switcher groups.*

ACTH: Adrenocorticotropic hormone; EC_{50}: 50% effective concentration; ESWL: Extracorporeal shock wave lithotripsy; HPA: Hypothalamic–pituitary–adrenal; M6G: Morphine-6-glucuronide; MAP: Mean arterial pressure; $PaCO_2$: CO_2 arterial pressure; PONV: Postoperative nausea or vomiting; VAS: Visual analogue scale.

Table 2. Association studies of *OPRM1* SNPs with the effects of opioid drugs (cont.).

Polymorphism	Opioid	Opioid effect	Result	Number of subjects	Ref.
A118G (cont.)	M6G	Pupil constriction	G-allele carriers > AA subjects (EC_{50} of M6G, $p < 0.05$)	AA, 6; AG, 5; GG, 1	[58]
	M6G	Electrical pain relief	Low M6G analgesia in G-allele carriers	AA, 12; AG, 6; GG, 0	[69]
	M6G	Electrical pain relief	AG subjects < AA subjects (M6G analgesia, $p < 0.01$)	AA, 12; AG, 4; GG, 0	[70]
		Respiratory depression	No (E_{max} and EC_{50} of acute hypoxic response)		
	Fentanyl	Preoperative analgesia	No (gastric response to fentanyl)	AA, 15; AG, 2; GG, 1	[71]
	Fentanyl	Labor analgesia	G-allele carriers < AA subjects (EC_{50} of fentanyl, $p < 0.01$)	AA, 150; AG, 62; GG, 11	[72]
	Fentanyl	Postoperative analgesia	G-allele carriers > AA patients (VAS score, $p < 0.05$)	AA, 99; AG, 66; GG, 24	[73]
		Side effects	G-allele carriers < AA patients ($PaCO_2$, $p < 0.05$)		
			GG patients < AA patients (time to awakening and extubation, $p < 0.05$)		
			No (respiratory depression)		
	Fentanyl	Thermal pain relief	G-allele carriers < AA subjects (pain threshold decrease, $p = 0.046$)	AA, 86; AG, 143; GG, 51	[40]
	Fentanyl	Postoperative analgesia	GG patients > A-allele carriers (fentanyl consumption, $p = 0.039$ or 0.01)	AA, 86; AG, 67; GG, 21	[42]
	Fentanyl	Labor analgesia	No (duration of fentanyl analgesia)	AA, 144; AG, 34; GG, 12	[74]
	Fentanyl/morphine	Postoperative analgesia	No (morphine requirement and duration of morphine analgesia)	AA, 78; AG, 22; GG, 3	
	Alfentanyl	Electrical pain relief	G-allele carriers < AA subjects (alfentanyl analgesia, $p < 0.05$)	AA, 10; AG, 4; GG, 6	[75]
		Chemical pain relief	GG subjects < A-allele carriers (alfentanyl analgesia, $p < 0.05$)		
		Side effects	GG subjects < A-allele carriers (respiratory frequency, $p < 0.01$)		
	Alfentanyl	ESWL pain relief	G-allele carriers > AA subjects (alfentanyl dose, $p < 0.01$)	AA, 72; AG, 24; GG, 3	[76]
			G-allele carriers > AA subjects (frequency of boluses, $p < 0.05$)		
	Levomethadone	Pupil constriction	G-allele carriers < AA subjects (miotic effect, $p < 0.001$)	AA, 40; AG, 8; GG, 3	[77]
	Buprenorphine	Heroin dependence treatment	G-allele carriers < AA patients (ACTH response, $p = 0.03$)	AA, 14; AG, 4; GG, 2	[78]
	Methadone	Opioid abuse treatment	No (methadone response)	AA, 177; AG, 57; GG, 4	[79]
	Some opioids	Postoperative analgesia	SNP × anger-out (analgesic consumption, $p < 0.05$)	AA, 37; AG, 10; GG, 1	[37]
	Some opioids	Chronic pain relief	G-allele carriers < AA patients (opioid dose, $p < 0.005$)	AA, 103; AG, 17; GG, 1	[65]
	Some opioids	Postoperative analgesia	GG patients > A-allele carriers (analgesic requirement, $p < 0.05$)	AA, 41; AG, 70; GG, 27	[80]
	Naltrexone	Alcoholic treatment	G-allele carriers < AA patients (rate of relapse, $p = 0.044$)	AA, 89; AG or GG, 41	[57]
			G-allele carriers > AA patients (time to relapse, $p = 0.040$)		
	Naltrexone	Alcoholic treatment	No (effects of naltrexone treatment)	AA, 59; AG or GG, 29	[81]
			G-allele carriers > AA patients (decrease of MAP, $p < 0.005$)		

†*The number of subjects combined the control and switcher groups.*

ACTH: Adrenocorticotropic hormone; EC_{50}: 50% effective concentration; ESWL: Extracorporeal shock wave lithotripsy; HPA: Hypothalamic–pituitary–adrenal; M6G: Morphine-6-glucuronide; MAP: Mean arterial pressure; $PaCO_2$: CO_2 arterial pressure; PONV: Postoperative nausea or vomiting; VAS: Visual analogue scale.

Table 2. Association studies of *OPRM1* SNPs with the effects of opioid drugs (cont.).

Polymorphism	Opioid	Opioid effect	Result	Number of subjects	Ref.
A118G (cont.)	Naltrexone	Alcoholic treatment	No (effects of naltrexone treatment)	AA, 16; AG, 6; GG, 3	[82]
	Naltrexone	Alcoholic treatment	No (rate and time to relapse)	AA, 148; AG or GG, 42	[83]
	Naltrexone	Alcoholic treatment	G-allele carriers < AA patients (craving for alcohol, $p < 0.05$)	AA, 25; AG, 14; GG, 1	[84]
			No (alcohol-induced stimulation, sedation or mood changes)		
	Naltrexone	Alcoholic treatment	No (effects of naltrexone treatment)	AA, 119; AG or GG, 54	[85]
	Naltrexone	Alcoholic treatment	G-allele carriers > AA patients (% of days abstinent, $p < 0.05$)	AA, 469; AG or GG, 135	[86]
			G-allele carriers < AA patients (% of heavy drinking days, $p < 0.05$)		
			G-allele carriers > AA patients (rate of good clinical outcome, $p = 0.005$)		
	Naltrexone	Alcoholic treatment	No (effects of naltrexone treatment)	AA, 75; AG or GG, 17	[87]
	Naltrexone	Alcoholic treatment	G-allele carriers > AA patients (time to relapse, $p = 0.014$)	AA, 25; AG or GG, 38	[88]
	Naltrexone	Alcoholic treatment	Haplotype (including A118G) × medication ($p = 0.03$)	Unknown	[89]
			G-allele carriers > AA patients (rate of good clinical outcome, $p = 0.006$)		
	Naltrexone	Alcoholic treatment	No (effects of naltrexone treatment)	AA, 89; AG, 16; GG, 3	[90]
	Naltrexone	Alcoholic treatment	No (naltrexone effects on impulsive choice ratio)	AA, –; AG, –; GG, –	[91]
	Nalmefene	Alcoholic treatment	No (effects of nalmefene treatment)	AA, 167; AG, 96; GG, 29	[92]
	Naloxone	HPA axis activation	G-allele carriers > AA subjects (cortisol response, $p < 0.05$)	AA, 29; AG, 9; GG, 1	[93]
			AG subjects > AA subjects (plasma ACTH response, $p < 0.05$)		
	Naloxone	HPA axis activation	G-allele carriers > AA subjects (cortisol response, $p < 0.05$)	AA, 24; AG, 5; GG, 1	[94]
			No (plasma ACTH response)		
	Naloxone	HPA axis activation	G-allele carriers > AA subjects (cortisol response, $p = 0.046$)	AA, 59; AG, 14; GG, 1	[95]
			No (plasma ACTH response)		
	Naloxone	HPA axis activation	G-allele carriers > AA subjects (cortisol response, $p < 0.05$)	AA, 6; AG, 5; GG, 1	[96]
			No (cortisol response)	AA, 7; AG, 8; GG, 2	
			G-allele carriers < AA subjects (plasma ACTH, $p = 0.04$)	AA, 13; AG, 13; GG, 3	
IVS1+C5143T	Morphine	Cancer pain relief	No (opioid switching)	CC, 100; CT, 55; TT, 1†	[55]
IVS1-C17823T	Morphine	Cancer pain relief	No (opioid switching)	CC, 80; CT, 70; TT, 6†	[55]
IVS2+G31A	Morphine	Cancer pain relief	No (morphine requirement)	GG, 83; GA, 16; AA, 0	[54]
	Morphine	Cancer pain relief	No (opioid switching)	GG, 129; GA, 27, AA, 0†	[55]
	Morphine/M6G	Pupil constriction	No (EC_{50} of opioids)	GG, 26; GA, 5; AA, 0	[62]
IVS2+C691G	Morphine	Cancer pain relief	No (morphine requirement)	CC, 39; CG, 46; GG, 14	[54]
	Morphine	Cancer pain relief	No (opioid switching)	CC, 34; CG, 72; GG, 50†	[55]
	Morphine/M6G	Pupil constriction	No (EC_{50} of opioids)	CC, 11; CG, 16; GG, 4	[62]
	Fentanyl	Preoperative analgesia	No (gastric response to fentanyl)	CC,4; CG, 14; GG, 0	[71]

†*The number of subjects combined the control and switcher groups.*

ACTH: Adrenocorticotropic hormone; EC_{50}: 50% effective concentration; ESWL: Extracorporeal shock wave lithotripsy; HPA: Hypothalamic–pituitary–adrenal; M6G: Morphine-6-glucuronide; MAP: Mean arterial pressure; $PaCO_2$: CO_2 arterial pressure; PONV: Postoperative nausea or vomiting; VAS: Visual analogue scale.

Table 2. Association studies of *OPRM1* SNPs with the effects of opioid drugs (cont.).

Polymorphism	Opioid	Opioid effect	Result	Number of subjects	Ref.
IVS2+C691G (cont.)	Some opioids	Postoperative analgesia	No (analgesic requirement)	CC, 87; CG, 45; GG, 6	[80]
	Naloxone	HPA axis activation	G-allele carriers > CC subjects (plasma ACTH response, p = 0.04) No (cortisol response)	CC, 13; CG or GG, 16	[96]
IVS3+G5953A	Some opioids	Postoperative analgesia	No (analgesic requirement)	GG, 112; GA, 25; AA, 1	[80]
IVS3+A8449G	Fentanyl	Postoperative analgesia	G-allele carriers > AA subjects (fentanyl requirement, p = 0.01)	AA, 219; AG, 60; GG, 1	[40]
	Some opioids	Postoperative analgesia	No (analgesic requirement)	AA, 116; AG, 21; GG, 1	[80]
IVS3-A1188G	Naltrexone	Alcoholic treatment	No (rate and time to relapse)	AA, 152; AG or GG, 50	[83]
	Nalmefene	Alcoholic treatment	No (nalmefene effects of treatment)	AA, 169; AG, 95; GG, 8	[92]
TAA+T1371C	Morphine	Cancer pain relief	No (opioid switching)	TT, 91; TC, 55; CC, 10†	[55]
TAA+A2109G	Some opioids	Postoperative analgesia	No (analgesic requirement)	AA, 116; AG, 21; GG, 1	[80]

†The number of subjects combined the control and switcher groups.
ACTH: Adrenocorticotropic hormone; EC_{50}: 50% effective concentration; ESWL: Extracorporeal shock wave lithotripsy; HPA: Hypothalamic–pituitary–adrenal; M6G: Morphine-6-glucuronide; MAP: Mean arterial pressure; $PaCO_2$: CO_2 arterial pressure; PONV: Postoperative nausea or vomiting; VAS: Visual analogue scale.

when they were conditioned for a long period of time (two sessions per day for 4–5 days) [103,104]. SNPs in the *OPRM1* gene might be expected to affect the susceptibility to substance dependence in humans. To date, numerous SNPs in the *OPRM1* gene have been analyzed for their involvement in the susceptibility to substance dependence (SUPPLEMENTARY TABLE 2) [26–31,34,110–150]. In studies of substance dependence or related traits, SNPs in exon 1 and intron 1 correlated with clinical traits with high frequency (number of analyses with positive correlation/total analyses: 0/7 [5′ flanking region], 0/5 [5′ UTR], 25/66 [exon 1], 26/47 [intron 1], 5/17 [intron 2], 0/1 [exon 3], 10/37 [intron 3], 3/11 [3′-UTR]). In the European and Japanese populations, a large LD block covers the region from exon 1 to intron 1, indicating that the LD block covering exon 1 and intron 1 in the *OPRM1* gene is critically involved in substance dependence and related traits.

Among the SNPs that have been analyzed with regard to substance dependence and related clinical traits, numerous studies showed that the A118G and IVS1+A21573G SNPs were associated with alcohol dependence or related traits. The G-allele frequency of the A118G SNP in alcohol dependence is higher or tends to be higher compared with nonalcoholic controls [111–113,121,124,125,130]. In contrast, some studies showed lower G-allele frequencies of the A118G SNP in alcohol dependence than nonalcoholic controls [119,120,128]. These controversial results in the A118G SNP for alcoholism might result from the various MAFs in different races/ethnicities, but this remains to be elucidated. The minor allele (G) frequency of the IVS+A21573G SNP in alcohol dependence was higher than in nonalcoholic controls [26].

In the case of opioid dependence, many studies have reported that the A118G and IVS1-T17286C SNPs were associated with opioid dependence. Similar to alcohol dependence, the G-allele frequency of the A118G SNP in opioid dependence was higher than in controls [114,133,137]. The minor allele (C) frequency of the IVS1-T17286C SNP in heroin dependence was higher than in controls [138].

The A118G and TAA+A5359G SNPs were also associated with tobacco dependence. In contrast to alcohol and opioid dependence, abstinence rates in G-allele smokers were higher than in AA smokers [139,141,142], and the number of cigarettes smoked in G-allele female smokers was smaller than in AA allele smokers [140], suggesting that the G-allele of the A118G SNP

is protective against smoking. In smokers, the minor allele (G) frequency of the TAA+A5359G SNP was smaller than in control subjects [27].

In these three types of substance dependence, previous studies have reported no significant association with the A118G SNP. A meta-analysis of 22 case–control studies failed to detect a significant association between A118G and substance dependence (odds ratio = 1.01, 95% CI: 0.86–1.19) [151]. The case–control studies examined by this meta-analysis examined dependence on several substances, including alcohol and opioids. Therefore, this meta-analysis did not strictly include specific substances. In another meta-analysis of case–control studies that examined the association between the A118G SNP and opioid dependence, no significant evidence was found for either dominant ($p = 0.810$) or additive ($p = 0.406$) effects of the A118G SNP on the risk for opioid dependence [152]. The pooled odds ratios and 95% CI derived from the eight European, six Asian, four African, two Hispanic, and one Native American samples were 1.20 (0.91–1.58), 0.93 (0.66–1.31), 0.99 (0.44–2.21), 2.60 (0.54–12.47) and 2.34 (0.68–8.03), respectively. The association with opioid dependence was not significant for any of these specific ancestral groups. However, the meta-analysis was designed to maintain statistical power greater than 97% for detecting additive effects and greater than 70% for detecting dominant or recessive effects with an odds ratio as small as 2.0. Therefore, if the odds ratio for the actual effect of the A118G SNP on the risk for opioid dependence was smaller than 2.0, then the meta-analysis would not have sufficient power for detecting the effects of the A118G SNP, indicating that further analyses are needed with specific ancestral samples.

Association of SNPs in the *OPRM1* gene with other disorders

SNPs in the *OPRM1* gene have been investigated for their involvement in various other disorders (Supplementary Table 3) [33,153–170]. The A118G SNP is the only variation that has been associated with susceptibility to disorders and related traits in numerous studies. Patients with idiopathic absence epilepsy showed high G-allele frequencies of the A118G SNP compared to control subjects [154,157]. The G-allele frequency in patients with schizophrenia was also higher than in control subjects [160]. By contrast, G-allele carriers, including normal subjects, with glucose tolerance and patients with impaired fasting glucose or Type 2 diabetes mellitus exhibited better glucose tolerance compared with AA homozygotes [161]. Furthermore, G-allele carriers in patients with painless diabetic foot ulcer were higher than in patients with painful diabetic foot ulcer [162]. In addition, a positive association was found between BMI and copy number of G-allele of the A118G SNP, and the G-allele frequency in the obesity groups was lower than in control groups in the Uyghur population [33]. The obese controls showed a lower G-allele frequency of the A118G SNP than patients with binge eating disorder [167]. These results indicate that the G-allele of the A118G SNP is a risk allele for epilepsy and schizophrenia, but it is protective for diabetes and obesity.

Effects of A118G SNP on MOP expression & function

Some *in vitro* and *in vivo* studies have reported the effects of the A118G SNP on opioid functions, including receptor binding and expression. One report found that the ligand-binding affinities of β-endorphin, morphine and naloxone for the MOP were not significantly different between wild-type and knockin mice (*Oprm1* A112G) [171]. Mice have four putative *N*-glycosylation sites in the MOP, and the number of these *N*-glycosylation sites is purportedly reduced to three in *Oprm1* A112G knockin mice. The human MOP has putatively five *N*-glycosylation sites, and the number of these *N*-glycosylation sites is reduced to four in 118G/G subjects. For this reason, the *Oprm1* A112G knockin mouse strain is not a suitable model for analyzing the effects of the A118G SNP in the human *OPRM1* gene. The effects of opioid antagonists have not been analyzed with regard to differences between G-allele and common allele homozygous carriers of the A118G SNP *in vitro*.

The binding affinity of β-endorphin, but not endomorphin-1, to the 118G variant of the MOP was higher than the common allelic form of the MOP in AV-12 cells [172]. No differences were observed, however, in morphine and [D-Ala(2),N-Me-Phe(4),Gly(5)-ol]-enkephalin (DAMGO) agonist binding between the 118G and common form of the MOP in COS cells [173]. Similarly, in HEK cells, no differences were observed in morphine, M6G, and β-endorphin agonist binding between the 118G and common form of the MOP [174]. A subsequent study, however, did not confirm these binding affinity results [175]. Kroslak *et al.* reported that the binding activity of morphine, DAMGO, and methadone but not β-endorphin were lower in

the 118G variant than in the common form of the MOP in both AV-12 and HEK cells. *In vivo*, in the somatosensory region of homo- and heterozygous carriers of the 118G variant, the efficacy of DAMGO was lower compared with homozygous carriers of the common allele, whereas the number of DAMGO binding sites was unaffected [176]. These discrepancies in the binding affinities of MOP agonists remain to be resolved. In heterozygous samples, the mRNA from the common allele was 1.5–2.5-fold more abundant than from the 118G variant allele [177]. A possible explanation for the reduced efficacy of opioid antagonists in 118G allele carriers may be the attenuation of MOP expression.

The expression of endogenous opioid peptides, including preproenkephalin and preprodynorphin, was reduced in numerous regions of heterozygous carriers of the 118G allele [178]. Alterations of endogenous opioid systems might underlie the enhanced susceptibility to alcohol and opioid dependence in 118G allele carriers.

Conclusion & future perspective

We have reviewed many *OPRM1* gene variations that have been identified and analyzed for their associations with pain sensitivity, opioid sensitivity and susceptibility to substance dependence and other disorders. These studies revealed significant associations between genetic variations, including the A118G SNP, with opioid sensitivity and susceptibility to substance dependence and other disorders (Figure 2). However, associations between variations in the *OPRM1* gene were not found in every analysis. Therefore, the pharmacogenetic significance of variations in the *OPRM1* gene is still being discussed. One explanation why statistical significance was not found in some analyses is that the MAFs of the variations are different among different races and ethnicities and lead to different effect sizes in the analyses. The MAFs of the A118G SNP vary among different races/ethnicities, which would be expected to affect the results of association studies. To further elucidate the genetic variability in the *OPRM1* gene that contributes to opioid efficacy and susceptibility to substance dependence, replication studies will be required in different races/ethnicities with sufficient samples for each effect size. In addition, although some functional analyses of the A118G SNP have been performed, the results of these studies are also controversial similarly to those of association studies. Molecular mechanisms underlying the relationships between genetic variations in the *OPRM1* gene and MOP expression and function should be elucidated for underlying and supporting the associations of these variations with clinical traits.

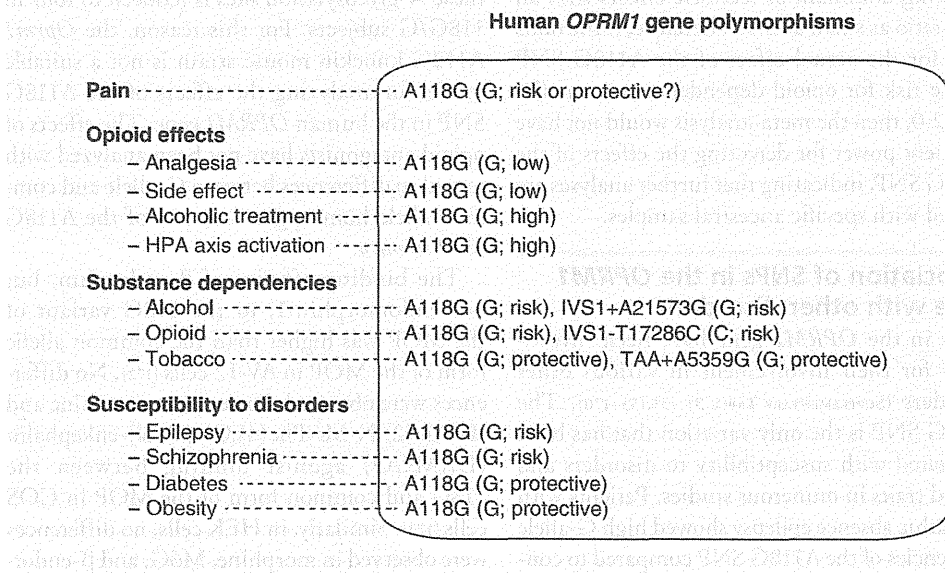

Figure 2. SNPs in the *OPRM1* gene associated with disorders and clinical conditions.
Numerous SNPs in the human *OPRM1* gene have been reported to be associated or not associated with pain sensitivity, opioid effects, drug dependence and susceptibility to other disorders. Only the SNPs that have been reported to be associated with disorders and clinical conditions in numerous studies are listed for each disorder and clinical condition.
HPA: Hypothalamic–pituitary–adrenal.